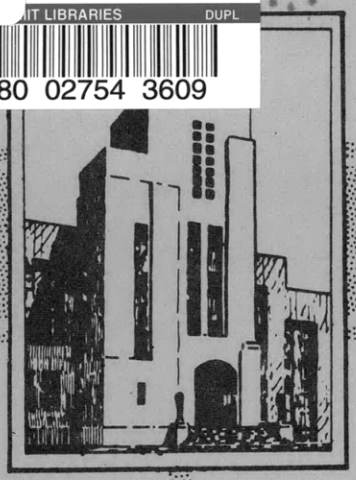

DEPARTMENT OF THE NAVY

DAVID TAYLOR MODEL BASIN

HYDROMECHANICS

AERODYNAMICS

STRUCTURAL MECHANICS

APPLIED MATHEMATICS

HYDROELASTIC INSTABILITY OF A CONTROL SURFACE

by

D. A. Jewell and Michael E. McCormick

HYDROMECHANICS LABORATORY

RESEARCH AND DEVELOPMENT REPORT

December 1961 Report 1442

HYDROELASTIC INSTABILITY

OF A CONTROL SURFACE

by

D. A. Jewell and Michael E. McCormick

December 1961

Report 1442

S-F013 02 01

TABLE OF CONTENTS

LIST OF FIGURES

LIST OF TABLES

NOMENCLATURE

a	Dimensionless distance from the midchord aft to the axis of rotation
b	Semi-chord length of foil
C	Damping coefficient
C_c	Critical damping coefficient
C(k)	Theodorsen's function of reduced frequency
f	Carriage excitation frequency
g	Artificial damping coefficient
h	Translational displacement of the axis of rotation (see Figure 4). When used as a subscript, h refers to the translational degree of freedom
h_o	Amplitude of the oscillatory translational displacement
I	Mass moment of inertia of the rotational assembly with respect to its axis
K_α	Linearized spring constant of the rotational degree of freedom
K_h	Linearized spring constant of the translational degree of freedom
k	Reduced frequency of vibration, $k = \omega b/U$
L	Unsteady lift
$L_{h,\alpha}$	Dimensionless, complex, unsteady lift coefficients
ℓ	Span length of the hydrofoil
M	Unsteady hydrodynamic moment about the axis of rotation
$M_{h,\alpha}$	Dimensionless, complex, unsteady moment coefficients
m	Mass of the system which vibrates in translation (including the rotational mass)
r_α	Dimensionless radius of gyration about the elastic axis

$$r_\alpha = (I/mb^2)^{\frac{1}{2}}$$

S_α First moment of mass aft of the rotational axis

U Velocity of the foil

x_α Dimensionless distance aft from the axis to the center of gravity of the rotational assembly; $x_\alpha = S_\alpha/mb$

Z Complex parameter used in flutter determinant, $Z = (\omega_\alpha/\omega)^2(1 + ig)$

α The rotational displacement of the foil about the axis of rotation. When used as a subscript, it refers to the rotational degree of freedom (see Figure 4)

α_o Amplitude of the oscillatory rotational displacement

μ Mass-density ratio; $\mu = m/\pi\rho b^2 \ell$

ρ Density of the liquid

Ω Ratio of the translational frequency to the rotational frequency, $\Omega = \omega_h/\omega_\alpha$

ω Circular frequency of the coupled vibration in water

ω_α Circular frequency of vibration in the rotational mode in air

ω_h Circular frequency of vibration in the translational mode in air

ABSTRACT

Initial evidence of flutter of a fully submergéd hydrofoil of small aspect ratio under controlled experimental conditions is presented. The influence of several primary parameters on flutter was investigated. Theodorsen's two-dimensional, unsteady flutter theory yielded flutter speed predictions in good agreement with experimental data. Based on the findings, some conditions under which flutter of displacement or hydrofoil craft could be anticipated are discussed.

INTRODUCTION

Since flutter is generally a destructive phenomenon, there is some concern about its possible occurrence on control-surfaces in water. This concern is warranted by the increasing use of hydrofoil configurations at high speed. Several investigators have expressed their views on this matter along with results of analytical studies in the new field of hydroelasticity. Reference 1 defines this new field of hydroelasticity.* In two of the first stability studies,[2,3] the classical translational and rotational degrees of freedom of hydrofoils were considered. Henry, et al.,[2] adapted theory from the field of aeroelasticity and investigated the static and oscillatory stability of an idealized, fully submerged foil. They concluded that flutter is very unlikely for the small values of the mass-density ratio μ typical of hydrofoils. In a parallel study, however, Abramson and Chu[3] were more concerned about the possibility of flutter.

---

*References are listed on page 24

Both studies indicated that there exists a minimum value of the mass-density ratio μ_{cr} below which flutter would not occur. The efforts of these early investigators were hampered by the lack of experimental flutter data with which to compare their theoretical predictions. In the only conclusive reports of flutter tests[4,5] in water available to them, no instability had been demonstrated. They, therefore, compared their theoretical results with results of experiments[6,7,8] in which light aeroelastic models were tested in wind tunnels using high-density gases. The comparisons which they made to determine the accuracy of flutter theory revealed certain inconsistencies which were not completely reconciled. Later, the results of Hilborne's study[9] became available. Hilborne produced flutter of solid, cantilevered, surface-piercing foils in a rotating-arm basin. He made predictions on the basis of an analysis which is seldom used in the United States. The predictions agreed with the experimental results, but the data reported were fragmentary and insufficient to enable one to make comparisons with the classical theory of Theodorsen, which is generally used in this country. It is known, however, that for one of Hilborne's foils, the value of the mass-density ratio was in the range considered by Henry, et al.[2] to be typical of hydrofoils. Hilborne's foils were simple flat plates, tapered at the leading and trailing edges and constructed of solid steel. His results* have been considered inconclusive for three reasons:

1. Circular path of travel of the foils.
2. Possible interference from the wake of a previous circuit.
3. Attendant cavitation at some speeds at which flutter was obtained.

In these early stability studies, no consideration was given to the possible destabilizing effects of a mass attached to the oscillating foil. Consideration of the stability of such an oscillatory system was prompted by the vibration problem encountered on USS FORREST SHERMAN (DD 931). The modes of vibration involved were identified by full-scale tests on destroyers

*Gruman Aircraft Engineering Corporation is now conducting tests with a linear towing path to verify Hilborne's results.

of the class as the three-noded horizontal hull mode, coupled with rotation of the rudders.[10] In this case, the stern vibrated in the horizontal athwartship direction and the rudders rotated as rigid bodies with respect to the stern about vertical axes through the rudder stocks. The hull-translation and rudder-rotation modes of vibration can be considered to correspond, respectively, to the translational and rotational modes of the classical flutter theory. An experimental study, conducted at the David Taylor Model Basin,[11] of a mass-foil system in water did not produce instability, but did indicate an approach to flutter. Jewell[12] discussed the possible destabilizing effect of an external mass attached to an oscillating foil. He pointed out that an additional mass, such as the effective mass of a ship hull, could increase the effective value of the mass-density ratio enough to permit or even promote flutter. McGoldrick[13] concluded that the DD 931 had suffered a flutter condition, although the problem was complicated by indications of cavitation on the ship's rudders. This problem is very interesting and controversial, as evidenced by McGoldrick's paper,[13] the discussions of the paper, and the author's reply.

The experimental study described herein is an extension of the work presented in Reference 11. The work was conducted at the Taylor Model Basin in an effort to provide documented data on flutter in water and to provide a firm basis for comparison with theoretical results. The experimental equipment and techniques are described, and the experimental flutter data are presented. Also provided are comparative theoretical data computed on the basis of a classical, two-dimensional, unsteady theory. This theory, originally derived by Theodorsen,[14] was used because it is well-known by experienced hydroelasticians and can be easily acquired by scientists or designers who are unacquainted with the field. This work is identified by Bureau of Ships Project Number S-F013 02 01, Task 1719.

EXPERIMENTAL EQUIPMENT

The flutter apparatus was basically the same as that used previously[11] at the Taylor Model Basin. The apparatus was mounted on a towing carriage which runs over the high-speed towing basin. The carriage is self-propelled and has a top speed of about 50 knots. The basin is 21 feet wide, over 2900 feet long, and is filled to a minimum depth of 10 feet. Figures 1, 2, and 3 show the following pertinent features of the apparatus:

1. The control surface is a relatively rigid, hollow hydrofoil (1a) with an NACA 0015 cross section, an 18-inch chord length 2b and an 18-inch span length ℓ.

2. The hydrofoil, vertical shaft (1b), cage (1c), top disk (1d), and sliding counterweights (2a) are all rigidly connected to form the rotational element with a vertical axis through the center of the top disk, the shaft axis, and the forward quarter chord of the foil.

3. The rotational degree of freedom is provided by allowing the rotational assembly to turn with respect to a strongback (3a) to which it is connected by flexures (3b). The mass moment of inertia of the rotational assembly with respect to the axis of rotation is denoted by I. The rotational flexures provide an elastic restoring moment with spring constant K_α. The natural frequency ω_α of the uncoupled rotational degree of freedom is given by $\omega_\alpha = \sqrt{K_\alpha/I}$.

4. The strongback and the entire rotational assembly can translate horizontally with respect to the towing carriage, to which they are connected by another set of flexures (3c). With this construction, the mass m, which oscillates in horizontal translation, includes the mass of the entire rotational assembly.

5. The degrees of freedom can be locked independently or the amplitudes of vibration can be limited by use of adjustable mechanical stops (1e).

6. The foil shaft passes through a hole in an 8-foot by 16-foot rectangular, horizontal surface plate shown in Figure 3 of Reference 11. The plate is used to minimize surface effects and serves as an end plate at the upper end of the hydrofoil. The surface plate is submerged 6 inches. There was approximately 1/16-inch clearance between the bottom of the surface plate and the top of the foil.

7. A "take-up" spring (1f) can be adjusted, within limits, to balance the steady lift force and keep the shaft positioned near the center of the hole in the surface plate. The translational flexures and the ajustable "take-up" spring provide an elastic restoring force with spring constant K_h.

8. The location of the center of gravity (c.g.) of the rotational element can be adjusted without changing the mass m or mass moment of inertia I about the axis of rotation by sliding the counterweights around the edge of the top disk of the rotational element. This provides a convenient means of varying the first moment of mass S_α.

The basic apparatus is denoted as Configuration A. Three other configurations — B, C, and D — are obtained by adding masses: to the top disk for B, to the strongback for C, and to both for D. These four inertia configurations are:

Configuration A is identical with that described in Reference 11 except that a wider range of values of the mass unbalance S_α are obtainable. This was accomplished by removing the forward damping coil (the black cylinder shown in Figure 1 above 1f but not in Figure 2) and replacing it with an equal mass at the same radius from the rotational axis. This new mass is part of the sliding counterweights (item 2a of Figure 2). The small differences between the values of the spring constants K_h and K_α given here and in Reference 11 are due to more careful calibration in the later studies. In this work, m, S_α, and I are defined as the structural inertias, whereas

in Reference 11 these quantities include the fluid added masses. The altered values of the uncoupled frequencies ω_h and ω_α (in air) reflect these revised definitions.

Configuration B was obtained by rigidly attaching a 71.5-lb weight (Item 2b of Figure 2) to the top disk of the apparatus. This mass increased the values of m and I and decreased the values of ω_h and ω_α. The mass was positioned to produce values of S_α much greater than those for Configuration A.

Configuration C was obtained by rigidly attaching the 71.5-lb weight to the strongback. This increased the value of m and decreased the value of ω_h from those for Configuration A and made them equal to their values for Configuration B. Since this mass was not attached to the rotational element, it did not affect the values of I, ω_α, or S_α, which are exactly the same as for Configuration A.

Configuration D was obtained by attaching the 71.5-lb weight to the top disk and a 51.5-lb weight to the strongback (Item 2c of Figure 2). This configuration is similar to Configuration B in that the values of I, ω_α, and S_α are the same. The 51.5-lb weight further increased the value of m and decreased the value of ω_h.

This oscillatory system can be considered as an idealized foil and mass, connected by translational and rotational springs as shown in Figure 4. The dimensionless parameter a is the ratio of the distance of the axis of rotation aft of midchord to the foil semi-chord length. The dimensioness distance from the axis of rotation to the center of gravity (c.g.) location is denoted by x_α. It is obtained by dividing the mass unbalance S_α by the product of the semi-chord b and the total translational mass m. Thus $x_\alpha = S_\alpha/mb$ and is positive for c.g. locations aft of the axis of rotation.

Strain gages were bonded to the translational and rotational flexures. The gage leads were wired to form four-arm bridges, and the amplified strain signals were recorded to indicate the vibratory displacements. Carriage vibrations were measured with accelerometers and were recorded. An interrupter device yielding one signal for every 10 feet of carriage travel was used in conjunction with timing signals to determine the carriage speed.

Limitations in the equipment complicated the experiment. Two pertinent limitations were:

1. Above 15 knots, the transverse displacement due to the steady lift force became so large that the foil shaft was pushed against the edge of the hole in the surface plate. Thus, the speed range was limited to those at which oscillatory displacements of measurable amplitude could be obtained. Except for this speed restriction, the limited displacements were not considered objectionable. In fact, the edges of the hole acted as stops and allowed data to be taken under unstable vibratory conditions without causing damage to the equipment.

2. At certain speeds, the frequency of vibratory sources on the carriage coincided with the frequency of the apparatus vibrations. A graph of carriage excitation frequencies is shown in Figure 5. Reference 11 contains a detailed discussion of these vibrations.

One other point should be mentioned here. During a static calibration it was noted that the translational displacement at the bottom of the foil was slightly greater than the displacement at the top of the shaft. This difference is attributed to the geometry of the translational flexures which gave the effect of a rotational displacement about a horizontal fore and aft axis located more than 20 feet above the foil. Since the maximum displacement at the tip of the foil was limited to about 0.5 in., the angular motion could be neglected and the foil motion considered to be transverse translation. Because of the slightly rotational motion of the foil in the translational degree of freedom, the value of the linearized spring constant K_h (the ratio of a statically applied force to the resulting

displacement) differed at the top and bottom of the foil. The value of K_h was therefore determined by computing $K_h = m\omega_h^2$, where ω_h is the measured frequency and m is the mass obtained by weighing.

The foil was hollow and was filled with water for both calibrations in air and testing in the basin. The increased damping due to the water in the foil was negligible, amounting to less than 0.001 of critical damping. With the above exceptions, the calibration procedures were the same as those described in Reference 11. The values of the dimensional constants and the dimensionless parameters of the apparatus are given in Tables 1, 2, and 3.

EXPERIMENTAL RESULTS

The specific objectives of the experiment were to:

1. Measure the oscillatory damping over the range of values of speed U and mass-unbalance S_α for as many configurations as were feasible.

2. Determine the quantitative relation between the reduced flutter speed $U_f/\omega_\alpha b$ and the dimensionless distance from the axis of rotation to the center of gravity x_α for each value of the mass-density ratio $\mu = m/\pi\rho b^2 \ell$ insofar as possible.

A secondary objective was to measure the frequency ω of vibration along with the damping. No attempt was made to determine the ratio of the amplitudes of vibration of the two degrees of freedom or to determine the phase relation between them.

The angle of attack of the foil was preset at 1.9 degrees. At this angle, incipient cavitation is expected to occur at the top of the foil at speeds over 25 knots. Since the speed was limited to approximately 15 knots for reasons previously noted, it is quite certain that the foil

TABLE 1

Constants Independent of Configuration

Symbol	Value	Dimensions
b	9.00	in.
K_α	3.72×10^4	lb-in./rad
K_h	894	lb/in.
ℓ	18.0	in.

TABLE 2

Parametric Values Dependent on Configuration

Symbol	Value				Dimensions
	A	B	C	D	
m	1.18	1.39	1.39	1.52	lb-sec^2/in.
I	49.1	55.6	49.1	55.6	lb-in.-sec^2
ω_α	27.5	25.9	27.5	25.9	rad/sec
ω_h	27.5	25.4	25.4	24.2	rad/sec
S_α	1.49	2.25	1.49	2.25	lb-sec^2
	1.63	2.40	1.63	2.40	
	1.77	2.54	1.77	2.54	
	1.88	2.66	1.88	2.66	
	1.99	2.77	1.99	2.77	
	2.16	2.86	2.16	2.93	
	2.26	2.93	2.26	3.04	
		3.04			

TABLE 3

Dimensionless Flutter Parameters

Symbol	Value			
a			-0.5	
	A	B	C	D
$\mu = m/\pi\rho b^2 \ell$	2.76	3.25	3.25	3.43
$r_\alpha = \sqrt{I/mb^2}$	0.717	0.703	0.660	0.672
$\Omega = \omega_h/\omega_\alpha$	1.00	0.981	0.924	0.934
$x_\alpha = S_\alpha/mb$	0.140	0.180	0.119	0.164
↓	0.154	0.192	0.130	0.175
	0.167	0.203	0.142	0.186
	0.177	0.213	0.150	0.194
	0.187	0.221	0.159	0.202
	0.203	0.229	0.173	0.214
	0.213	0.234	0.181	0.222
		0.243		

was fully wetted during these tests. The adjustable stop for the translational degree of freedom was set to coincide with the maximum displacement permitted by the size of the hole in the surface plate. A short-circuit indicator was installed on this stop for nearly all of the stability runs, and the interrupted signal, if it occurred, was recorded with the other data. There was no indication that the rotational displacement was limited by any mechanical stops. Each stability test was conducted with the carriage moving at essentially constant speed.

Sample records of the vibration data are shown in Figure 6. Figure 6a is a complete record showing carriage vibrations, and speed and time signals as well as unstable system oscillations. The nature of each of the three types of oscillatory stability is clearly shown:

Figure 6b Stable oscillation (positively damped).
Figure 6c Neutrally stable oscillation (undamped).
Figure 6a Unstable oscillation (negatively damped).

The unstable vibrations were evidently self-excited since they required no excitation other than the normal background vibrations of the carriage. It was necessary to stop these vibrations externally and to allow them to increase in amplitude again in order to measure the rate of increase for the determination of the magnitude of the (negative) damping. Otherwise, the unstable oscillations would continue with the amplitude allowed by the stop until the end of the run when the forward speed was decreased. When the vibrations were stable or neutrally stable it was necessary to excite them by striking the apparatus with a timber. The amplitude of the oscillations would then instantaneously become greater than the background level, and then decrease exponentially in the case of stable vibrations or remain constant in the case of neutrally stable vibrations.

In reducing the data, only those oscillations whose amplitudes were greater than the background level and less than those permitted by the stop were considered. Any small variations in the amplitude envelope were neglected by fairing through the amplitude envelopes. The measured

logarithmic damping decrements (or increments) for each degree of freedom were converted to dimensionless damping ratios in the same manner as for a single degree of freedom system:

$$(C/C_c)_{translation} = \frac{1}{2\pi n} \ln\left(\frac{h_o(t)}{h_o(t+n\tau)} \right), \text{ or}$$

$$(C/C_c)_{rotation} = \frac{1}{2\pi n} \ln\left(\frac{\alpha_o(t)}{\alpha_o(t+n\tau)} \right)$$

where

C	is the effective linearized damping coefficient
C_c	is the effective critical damping coefficient of the foil system
n	is the number of periods between the measured amplitudes
$h_o(t)$	is the translational amplitude at time t
$\alpha_o(t)$	is the rotational amplitude at time t
τ	is the period of oscillation

The values of the damping ratios and frequencies of vibration ω are plotted in Figure 7 as functions of U for each value of S_α. All data shown in Figure 7 were obtained for oscillations about a preset angle of attack of $\alpha_s = 1.9$ degrees except for Configuration B at $S_\alpha = 2.25$ lb-sec^2, shown in Figure 7c. In this case, the preset angle of attack was 0.6 degree. Data for which the frequency of vibration coincided with a carriage excitation frequency are marked with flags. Often the effect of frequency coincidence was to reduce the apparent value of the damping ratio.

The experimental critical flutter speeds U_f and frequencies ω_f were obtained as the values for zero damping from the damping curves. No critical conditions were observed for Configuration C and only one case was observed for Configuration A. Unfortunately, for Configuration A at $S_\alpha = 2.26$ lb-sec^2, the flutter frequency coincided with a carriage excitation frequency. The authors believe, however, that the indicated critical flutter speed is approximately correct.

For Configuration B, where $S_\alpha = 2.25$ lb-sec^2, the critical flutter speed was obtained by extrapolation of the data; no actual instability was observed. For Configuration B, where $S_\alpha = 2.40$, 2.54, and 2.66 lb-sec^2, and for Configuration D, where $S_\alpha = 2.77$ and 2.93 lb-sec^2, data were obtained for only a limited range of speeds near U_f. Accurate interpolation of these damping data to determine U_f was somewhat difficult. These values of U_f are therefore considered to be less accurate (within 10 percent) than any other values. The most accurate values of U_f were obtained for the following values of S_α: For Configuration B, $S_\alpha = 2.77$, 2.86, 2.93, and 3.04 lb-sec^2, and for Configuration D, $S_\alpha = 3.04$ lb-sec^2. The accuracy of these values is estimated to be within 5 percent.

The experimentally determined values of U_f and ω_f are listed in Table 4. The dimensionless values of the critical flutter speed will be shown later when the experimental data are compared with the theoretical data.

TABLE 4

Critical Flutter Speed and Frequency Values

for Each Configuration

		Experimental		Theoretical	
Config.	S_α lb-sec^2	U_f in./sec	ω_f rad/sec	U_f in./sec	ω_f rad/sec
A	2.26	301	30.0	273	30.6
B	2.25	300	28.2	270	28.0
↓	2.40	252	28.6	256	28.3
	2.54	264	28.5	244	28.5
	2.66	244	28.8	239	28.7
	2.77	253	28.6	235	28.9
	2.86	250	29.2	231	29.1
	2.93	239	29.4	230	29.2
	3.04	229	29.8	227	29.4
D	2.77	300	27.9	266	27.8
↓	2.93	278	28.1	258	28.0
	3.04	274	28.2	254	28.2

THEORY

The analysis of the stability of the oscillatory system used in the experiment was based on the classical two-dimensional flutter analysis of aeroelasticity developed by Theodorsen.[14] This analysis is appropriate for this system since the modes of vibration are very well defined and the foil oscillates as a rigid body with elastic restraints. The use of the two-dimensional expressions for foils of small aspect ratio is not new in this work. For example, Widmayer, et al.[15] compared their experimental flutter data with reference theoretical values obtained from two-dimensional theory. Their models had aspect ratios ranging from 2 to 13. For aspect ratios from 2 to 6, the two-dimensional theory predicted lower flutter speeds than those obtained experimentally. The difference increased as the aspect ratio decreased. Admittedly, the two-dimensional flutter theory can be somewhat inaccurate when used for low aspect ratio foils; however, it should be recognized that a slight underestimation of the flutter speed is desirable. Abramson[16] used two-dimensional hydrodynamic expressions in a study of the stability of a control surface on a submarine. Woolston and Castile[6] also used such expressions in their study. Although they dealt with aspect ratios from 4 to 8, they showed that the use of the three-dimensional expressions produced only slightly different predictions of the critical speeds. Reference 17 stated that three-dimensional effects are less significant at high values of the reduced frequency, e.g., those obtained in the present case, than at low values. Due to the complexity of the three-dimensional expressions, their use often results in an uneconomical expenditure of effort.

The equations of motion for the system shown in Figure 4 can be written:*

$$m\ddot{h} + S_\alpha \ddot{\alpha} + K_h h = - L \qquad [1]$$

$$S_\alpha \ddot{h} + I\ddot{\alpha} + K_\alpha \alpha = M \qquad [2]$$

*Dots indicate differentiation with respect to time.

where h is the translational displacement of the axis of rotation from the foil equilibrium position,

α is the angular displacement of the foil from its equilibrium position, and

L and M are the unsteady hydrodynamic lift force and moment referred to the axis of rotation.

Structural damping forces have been neglected in the derivation of these equations. A brief survey of aeroelastic flutter calculations indicates that inclusion of such forces is seldom necessary . For the subject apparatus, at rest, the damping ratio C/C_c in water is less than 0.01 for each uncoupled degree of freedom.

If simple harmonic motion is assumed, $h = h_o e^{i\omega t}$, $\alpha = \alpha_o e^{i\omega t}$, and Equations [1] and [2] can be written:

$$-m\omega^2 h - S_\alpha \omega^2 \alpha + m\omega_h^2 h = -L \qquad [3]$$

$$-S_\alpha \omega^2 h - I\omega^2 \alpha + I\omega_\alpha^2 \alpha = M \qquad [4]$$

The expressions used to represent the oscillatory lift force L and moment M are those applicable to two-dimensional foils. The foil used in the experiment was of unit aspect ratio; however, with the surface plate at one end, the effective aspect ratio was very nearly two. It is intended to demonstrate the validity of the use of the two-dimensional expressions a posteriori when the theoretical data are compared with the experimental data.

The two-dimensional, unsteady lift and moment expressions given by Theodorsen[14] were multiplied by the length of the foil ℓ to obtain the total unsteady hydrodynamic loading expressions

$$L = \pi\rho b^2 \ell[\ddot{h} + U\dot{\alpha} - \underline{a}b\ddot{\alpha}] + 2\pi\rho b\ell UC(k)[\dot{h} + U\alpha + (\tfrac{1}{2} - \underline{a})b\dot{\alpha}] \qquad [5]$$

$$M = \pi\rho b^3 \ell[\underline{a}\ddot{h} - (\tfrac{1}{2} - \underline{a})U\dot{\alpha} - (1/8 + \underline{a}^2)b\ddot{\alpha}]$$
$$+ 2\pi\rho b^2 \ell UC(k)(\underline{a} + \tfrac{1}{2})[\dot{h} + U\alpha + (\tfrac{1}{2} - \underline{a})b\dot{\alpha}] \qquad [6]$$

which can also be written as

$$L = -\pi\rho b^3 \ell\omega^2 \{L_h h/b + [L_\alpha - L_h(\tfrac{1}{2} + \underline{a}]\alpha\} \qquad [7]$$

$$M = \pi\rho b^4 \ell\omega^2 \{[M_h - L_h(\tfrac{1}{2} + \underline{a})]h/b \qquad [8]$$
$$+ [M_\alpha - (L_\alpha + M_h)(\tfrac{1}{2} + \underline{a}) + L_h(\tfrac{1}{2} + \underline{a})^2]\alpha\}$$

where h and α have been assumed to vary sinusoidally with respect to time.

In these last expressions, Equations [7] and [8], the notation of Smilg and Wasserman[18] was used:

$$L_h = 1 - 2iC(k)/k$$
$$L_\alpha = \tfrac{1}{2} - [1 + 2C(K)]i/k - 2C(k)/k^2 \qquad [9]$$
$$M_h = \tfrac{1}{2}$$
$$M_\alpha = 3/8 - i/k$$

Here

$$k = \frac{\omega b}{U} \quad \text{and} \quad C(k) = \frac{H_1^{(2)}(k)}{H_1^{(2)}(k) + iH_o^{(2)}(k)} \qquad [10]$$

where $H_1^{(2)}$ and $H_o^{(2)}$ are Hankel functions of the second kind, the first

and zero orders, respectively.

Since the axis of rotation of the TMB flutter apparatus is located at the forward quarter-chord, $\underline{a} = -\frac{1}{2}$ and several of the hydrodynamic terms in Equations [7] and [8] are zero. Substitution of these simplified expressions into Equations [3] and [4] and division of Equation [3] by $\pi\rho b^3 \ell\omega^2 e^{i\omega t}$ and Equation [4] by $\pi\rho b^4 \ell\omega^2 e^{i\omega t}$, gives the following flutter equations in terms of the dimensionless parameters μ, Ω, x_α, and r_α and the dimensionless amplitudes h_o/b and α_o:

$$\{\mu[1 - \Omega^2(\omega_\alpha/\omega)^2] + L_h\}h_o/b + \{x_\alpha\mu + L_\alpha\}\alpha_o = 0 \qquad [11]$$

$$\{\mu x_\alpha + M_h\}h_o/b + \{\mu r_\alpha^2[1 - (\omega_\alpha/\omega)^2] + M_\alpha\}\alpha_o = 0 \qquad [12]$$

These equations express relations between the various parameters at the critical flutter speed and frequency. To investigate the stability of the system under conditions other than critical, a damping coefficient g was used. The quantity $(\omega_\alpha/\omega)^2$ in Equations [11] and [12] is replaced by the dimensionless quantity

$$Z = (\omega\alpha/\omega)^2(1 + ig) \qquad [13]$$

where g can be interpreted as representing the amount of damping required to produce neutral stability.

The homogeneous simultaneous equations, Equations [11] and [12], have nontrivial solutions only when the determinant of the coefficients of h_o/b and α_o is zero:

$$\mu^2 r_\alpha^2 \Omega^2 Z^2 - [\mu\Omega^2(\mu r_\alpha^2 + M_\alpha) + \mu r_\alpha^2(\mu + L_h)]Z - [\mu x_\alpha + M_h][\mu x_\alpha + L_\alpha] + [\mu + L_h][\mu r_\alpha^2 + M_\alpha] = 0 \qquad [14]$$

This quadratic can be solved for the complex quantity Z and, hence, the damping coefficient g and the frequency ω. In the solution of this complex quadratic, values of ω and g are computed for assumed values of k. The corresponding speeds are then found from $U = \omega b/k$.

The values of g and ω are plotted as functions of U for each set of values of μ, r_α, x_α, and Ω in Figure 8. The value of g is negative for stable oscillations and positive for unstable oscillations. As usual in flutter calculations, only one of two roots of the complex quadratic indicates an instability. Of the two roots, the values of g and ω shown in Figure 8 correspond to the mode of vibration which is unstable for sufficiently large values of x_α. The theoretical values of U_f and ω_f were obtained by interpolation (corresponding to g = 0) in the same manner as the experimental values.

DISCUSSION

Although the damping parameters g and C/C_c are related, they are different in concept; therefore no quantitative comparison of their values is attempted. It is noted, however, that the corresponding damping versus speed curves are qualitatively similar. The reader can compare values of the experimental and theoretical frequencies, but this comparison is considered to be of secondary interest at present. Of utmost importance here is a quantitative comparison of the experimental and theoretical values of the flutter speed. For this purpose, U_f is shown plotted against S_α for each configuration in Figure 9. Table 4 also lists U_f and ω_f for each configuration. In addition, the reduced flutter speed parameter $U_f/\omega_\alpha b$ is shown as a function of the dimensionless distance from the axis of rotation to the center of gravity x_α in Figure 10. It is noteworthy that flutter occurred at the relatively low speeds of 11.5 to 16 knots.

It is clear from Figures 9 and 10 that an increased value of S_α or

x_α results is a decreased critical flutter speed for the range of values of system parameters (μ, r_α, Ω) considered. This destabilizing effect of increasing S_α is common knowledge among aeroelasticians. The analytical results agree with the experimental results in showing this trend. The critical flutter speed can be larger for much larger values of S_α and can remain finite for negative values of S_α. The predicted critical flutter speeds are either conservative (a maximum of 12 percent less than the experimental critical speed) or lie within the experimental error. In fact, only three of the theoretical critical flutter speeds differ from the experimental speeds by more than the estimated experimental accuracy. The authors believe that the results of the comparison just stated definitely justify the use of the unsteady two-dimensional flutter theory for the values of μ, a, and k involved in this study to determine critical flutter speeds of similar configurations.

In these results, the reduced frequency k at the critical flutter speed and frequency ($\omega_f b/U_f$) ranges from a theoretical value of 0.833 for Configuration B, where S_α = 2.54 lb-sec^2, to an experimental value of 1.17 for Configuration B, where S_α = 3.04 lb-sec^2. These are very high values with respect to those prevalent in aeroelasticity where typical values of k are of the order of 0.1. It was reported[17] that several two-dimensional aerodynamic terms in Theodorsen's expressions for the unsteady lift and moment differ from experimental values for k above 0.4. Therefore, one might expect poor agreement between theoretical and experimental flutter results. In the current study, however, the theoretical predictions shown in Figures 9 and 10 are in good agreement with the experimental flutter speeds and frequencies. These results appear to reinforce the statement made previously that three dimensional effects are less significant at high values of the reduced frequency than at low values.

Since both r_α and Ω were changed with μ in this experiment, no conclusions concerning the effect of μ on the U_f trends could be obtained. Although the predicted and experimental speeds agree, there remains the possibility that the flutter theory used herein would yield unconservative critical speed predictions for lower values of μ. This would

correspond to the inaccuracy of flutter predictions of Woolston and Castile[8] for values of μ near μ_{cr}. Values of μ_{cr} were computed for two values of x_α for Configuration B. For $x_\alpha = 0.192$, $\mu_{cr} = 2.44$ and for $x_\alpha = 0.243$, $\mu_{cr} = 1.93$, as shown in Figure 11. The experimental value for μ (3.25) was too much larger than μ_{cr} to indicate the accuracy of the theoretical prediction of U_f near μ_{cr}. Due to the limitations of the existing flutter apparatus, the authors could not investigate this matter. Mr. C. J. Henry of the Davidson Laboratory is investigating this U_f dependence on μ both by experiment in water and by analysis.

It appears appropriate to consider what this and earlier studies indicate concerning the possibility of flutter occurrence on displacement vessels and hydrofoil craft. The control surfaces of ships, such as the DD 931 rudders, are usually mass balanced; that is, x_α is nearly equal to zero. Previous studies show that flutter occurs at relatively high values of the reduced flutter speed $U_f/\omega_\alpha b$ for $x_\alpha = 0$; see Figure 12, taken from Reference 19. In addition, the flutter speed is relatively high for large values of μ, such as $\mu = 36$, which is the effective value calculated for DD 931. This indicates that until speeds of surface ships or submarines are increased significantly, they are not in danger of hull-control-surface flutter, especially where no free-surface or cavitation effects are involved. In spite of this, both the experimental results and Figures 12 d, e, and f show that flutter could occur at low speed on a configuration where the center of gravity of a control surface lies somewhat aft of the axis of rotation. In this case, the minimum flutter speed occurs for a value of Ω near unity, which is the value derived for the DD 931.

When the possibility of hydrofoil-craft flutter is considered, the indication is more serious. Although the value of μ is slightly below μ_{cr} for ordinary foil sections, the inclusion of propeller nacelles or large end plates on hydrofoil configurations could effectively increase μ to values above μ_{cr}. In this case, hydrofoil craft could be susceptible to flutter because of their high speed and because of the many possible coupled modes of vibration of the flexible foils, struts, control surfaces, and hull. Using aeroelastic experience with troublesome "Tee Tail"

flutter problems as a guide, the combination of a horizontal foil attached to a vertical strut would be particularly susceptible to flutter. In any case, if flutter occurs at a value of μ slightly greater than μ_{cr}, it will occur near the least possible critical speed, as shown in Figure 12.

The pertinent points can be summarized as follows:

1. Flutter can occur on displacement vessels at high speeds in the coupled hull-bending, control-surface-rotation mode of vibration for sufficiently large values of x_α. The critical flutter speed is reduced for values of Ω near unity.

2. On hydrofoil craft, if coupling occurs between any of the many possible vibratory modes and if the effective value of μ is greater than μ_{cr}, then flutter is quite probable.

It should be emphasized that these experiments utilize idealized systems representing specified modes and couplings. Other vibratory modes and couplings must be studied, together with the special effects of the free surface, cavitation, and waves. These last three phenomena introduce new boundary conditions which distinguish hydroelastic from aeroelastic phenomena. Analytical studies of these effects[20] indicate that cavitation will seriously worsen the flutter problem. The only experimental work on these effects known now is that of Hilborne.[9] Until the influences of these special effects are determined experimentally, the seriousness of the threat of flutter to naval configurations will remain in doubt. It is therefore recommended that experimental studies be pursued to cover the wide range of current and projected hydrofoil operating conditions.

CONCLUSIONS

Flutter of a control surface has been definitely demonstrated in water. Although flutter is generally considered to be a high-speed phenomenon, it was produced at the relatively low speed of 11.5 knots. A simple flutter theory was shown to be adequate to predict the phenomenon in this study but some doubt remains about its accuracy for other structural configurations and flow conditions.

These results indicate that flutter could be an extremely serious hydro-elastic problem, particularly for hydrofoil craft.

ACKNOWLEDGMENTS

The authors wish to thank Mr. A. Taplin of the Bureau of Ships and Dr. M. C. Harrington and Mr. R. T. McGoldrick of the David Taylor Model Basin for their encouraging efforts. Without their foresight and support, this work would not have been possible. We are also grateful to Messrs. J. A. Luistro and T. J. Langan of the Model Basin for their assistance. Acknowledgment is also due to Messrs. D. Coder and H. Haller who assisted with the theoretical computations.

REFERENCES

1. Heller, S. R. and Abramson, H.N. , "Hydroelasticity: A New Naval Science," Transactions of the American Society of Naval Engineers, Vol. 71, pp. 205-209 (May 1959).

2. Henry, C. J., Dugundji, J. and Ashley, H., "Aeroelastic Stability of Lifting Surfaces in High Density Fluids," Journal of Ship Research, Vol. 2, pp. 10-21 (Mar 1959).

3. Abramson, H. N., and Chu, W. H., "A Discussion of the Flutter of Submerged Hydrofoils," Journal of Ship Research, Vol. 3, pp. 5-13 (Oct 1959).

4. Henry, C. J., "An Investigation by Analysis and Experiment of the Flutter Phenomenon in High Speed Hydrofoils," M. S. Thesis, Massachusetts Institute of Technology (Jun 1957).

5. Herr, R. W. "A Study of Flutter at Low Mass Ratios with Possible Application to Hydrofoils," National Aeronautics and Space Administration TN D-831 (May 1961).

6. Woolston, D. S. and Castile, G. E., "Some Effects of Variations in Several Parameters Including Fluid Density on the Flutter Speed of Light Uniform Cantilever Wings," National Advisory Committee for Aeronautics TN 2558 (Dec 1951).

7. Deyst, J. J., "An Experimental Investigation of the Flutter Characteristics of Low Density Wings," B. S. Thesis, Massachusetts Institute of Technology (Jun 1958).

8. Pratt, R. M., "An Investigation of the Flutter of Low Density Wings," S. M. Thesis, Massachusetts Institute of Technology (Jan 1952).

9. Hilborne, D. V., "The Hydroelastic Stability of Struts," Admiralty Research Laboratory/ R1/G/HY/5/3, Teddington, Middlesex,

England (Nov 1958).

10. Antkowiak, E. T., "Hull Vibrations in the DD931 Class Destroyer," Boston Naval Shipyard Evaluation Report R-10 (20 Aug 1956).

11. McGoldrick, R. T. and Jewell, D. A., "A Control-Surface Flutter Study in the Field of Naval Architecture," David Taylor Model Basin Report 1222 (Sep 1959).

12. Jewell, D. A., "A Note on Hydroelasticity," Journal of Ship Research, Vol. 3, pp. 9-12 (Mar 1960).

13. McGoldrick, R. T., "Rudder-Excited Hull Vibration on USS FORREST SHERMAN (DD 931) (A Problem in Hydroelasticity)," Transactions Society of Naval Architects and Marine Engineers, pp. 341-385 (1959). Also David Taylor Model Basin Report 1431 (Jun 1960).

14. Theodorsen, T. "General Theory of Aerodynamic Instability and the Mechanism of Flutter," National Advisory Committee for Aeronautics Report 496 (1935).

15. Widmayer, E. Jr., Lauten, W. T., Jr., and Clevenson, S. A., "Experimental Investigation of the Effect of Aspect Ratio and Mach Number on the Flutter of Cantilever Wings," National Aeronautics and Space Administration TN D-229 (Apr 1960).

16. Abramson, H. N., "An Exploratory Study of the Flutter Characteristics of the Fairwater Planes of the SSN 585 (SKIPJACK)," Southwest Research Institute Technical Report 5 (Dec 1959).

17. Bisplinghoff, R. L., Ashley, H., and Halfman, R. L., "Aeroelasticity," Addison-Wesley, Cambridge (1955).

18. Smilg, B. and Wasserman, L. S., "Application of Three-Dimensional Flutter Theory to Aircraft Structures," Air Force Technical Report 4798 (Jul 1942).

19. Theodorsen, T. and Garrick, I. E., "Mechanism of Flutter - A Theoretical and Experimental Investigation of the Flutter Problem," National Advisory Committee for Aeronautics Report 685 (1940).

20. Kaplan, Paul and Henry, C. J. "A Study of the Hydroelastic Instabilities of Supercavitating Hydrofoils," Journal of Ship Research, Vol. 4, pp. 28-38 (Dec 1960).

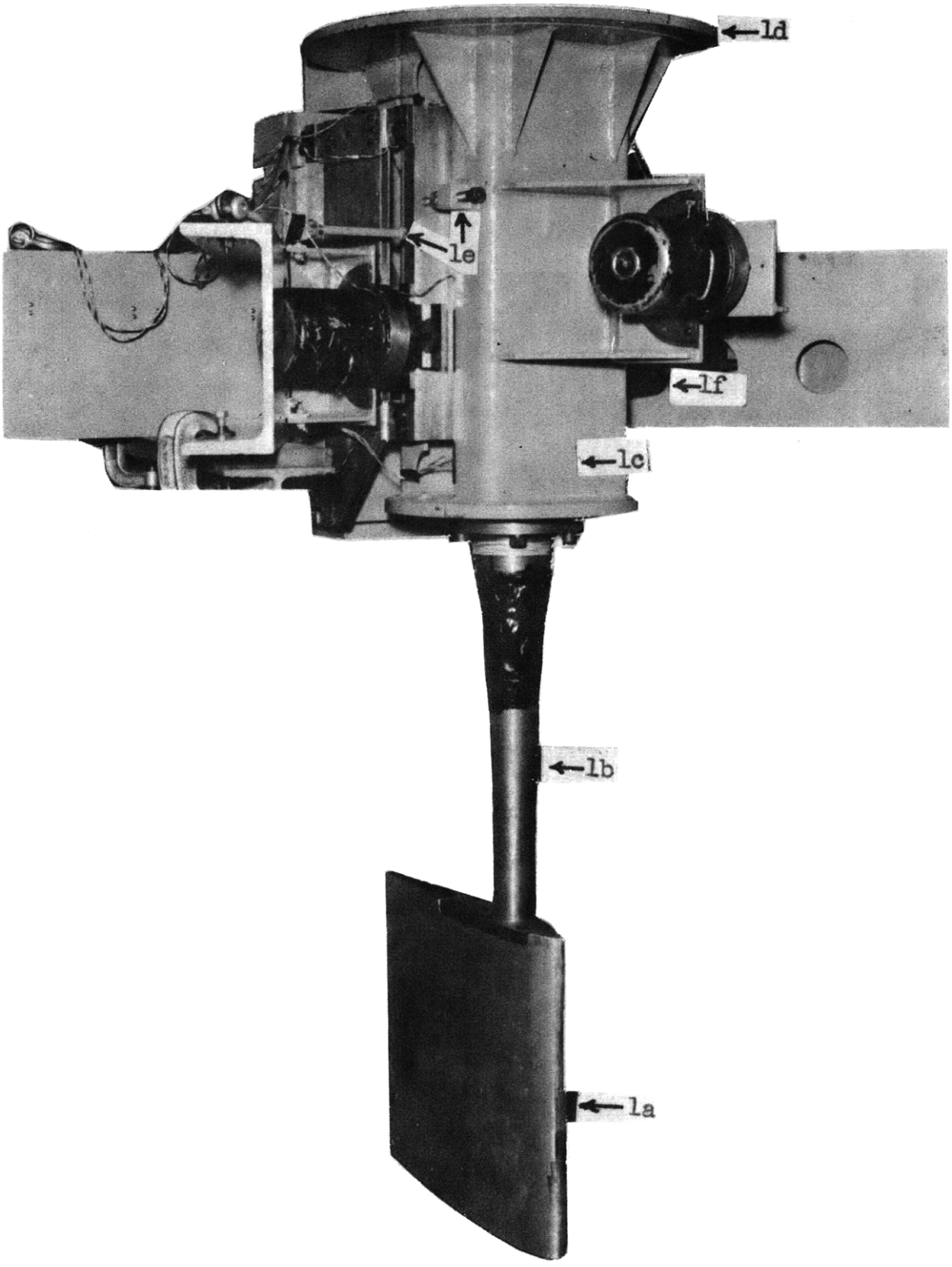

Figure 1 – TMB Flutter Apparatus

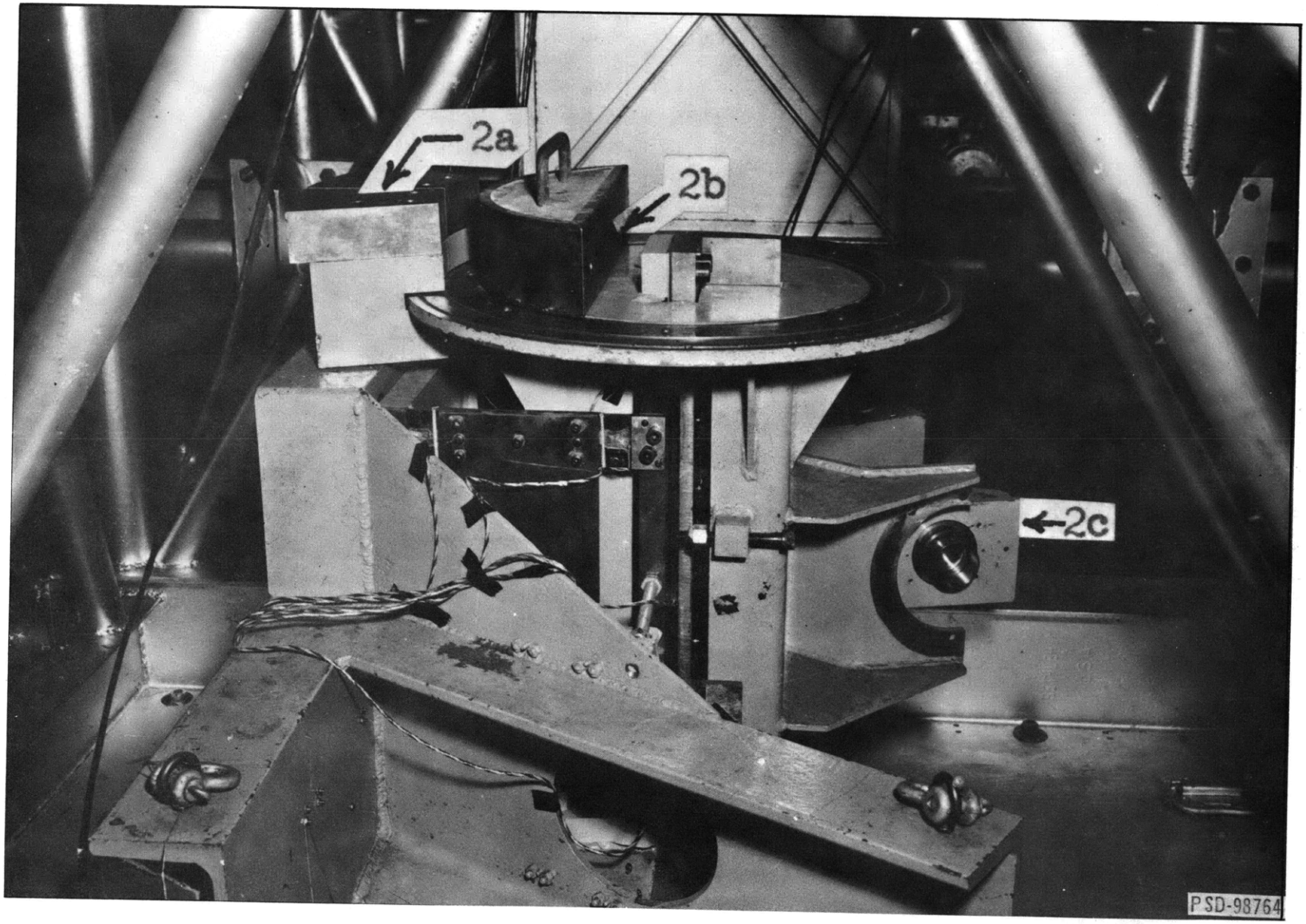

Figure 2 – Close-Up View of TMB Flutter Apparatus

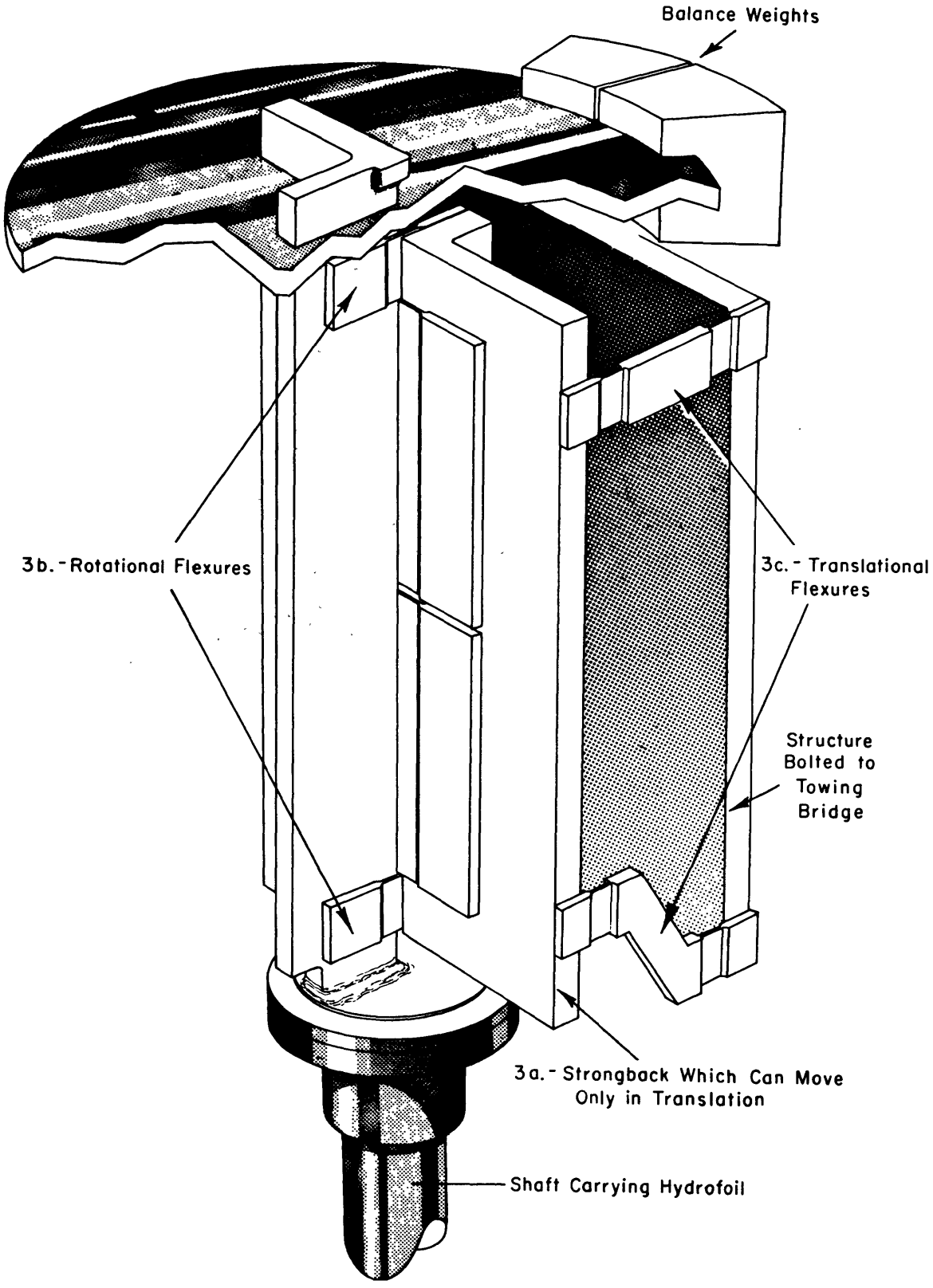

Figure 3 – Sectional Elevation of TMB Flutter Apparatus

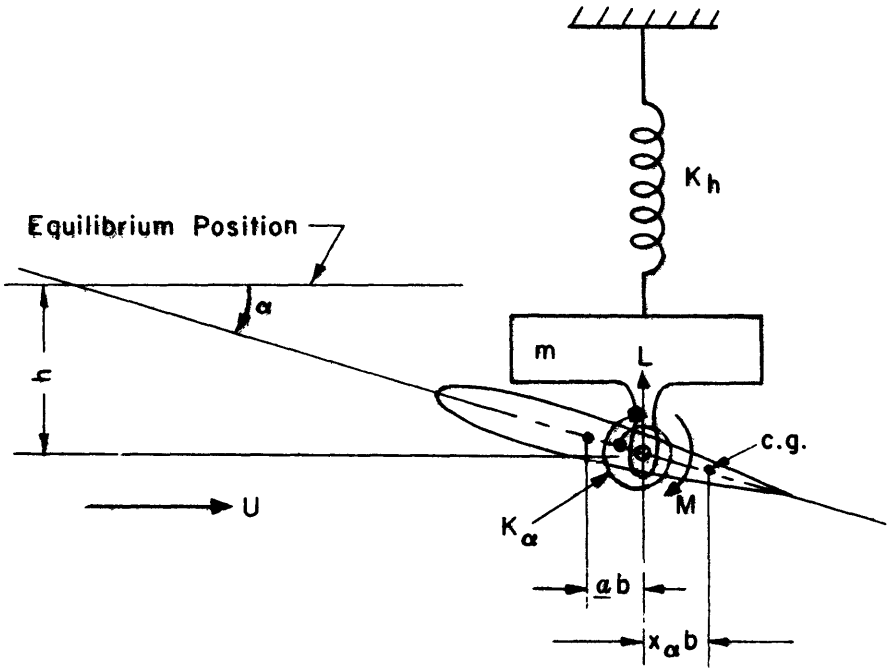

Figure 4 – Idealized Foil-Mass System

(This figure was prepared based on a concept suggested by Mr. C. Henry in a private conversation.)

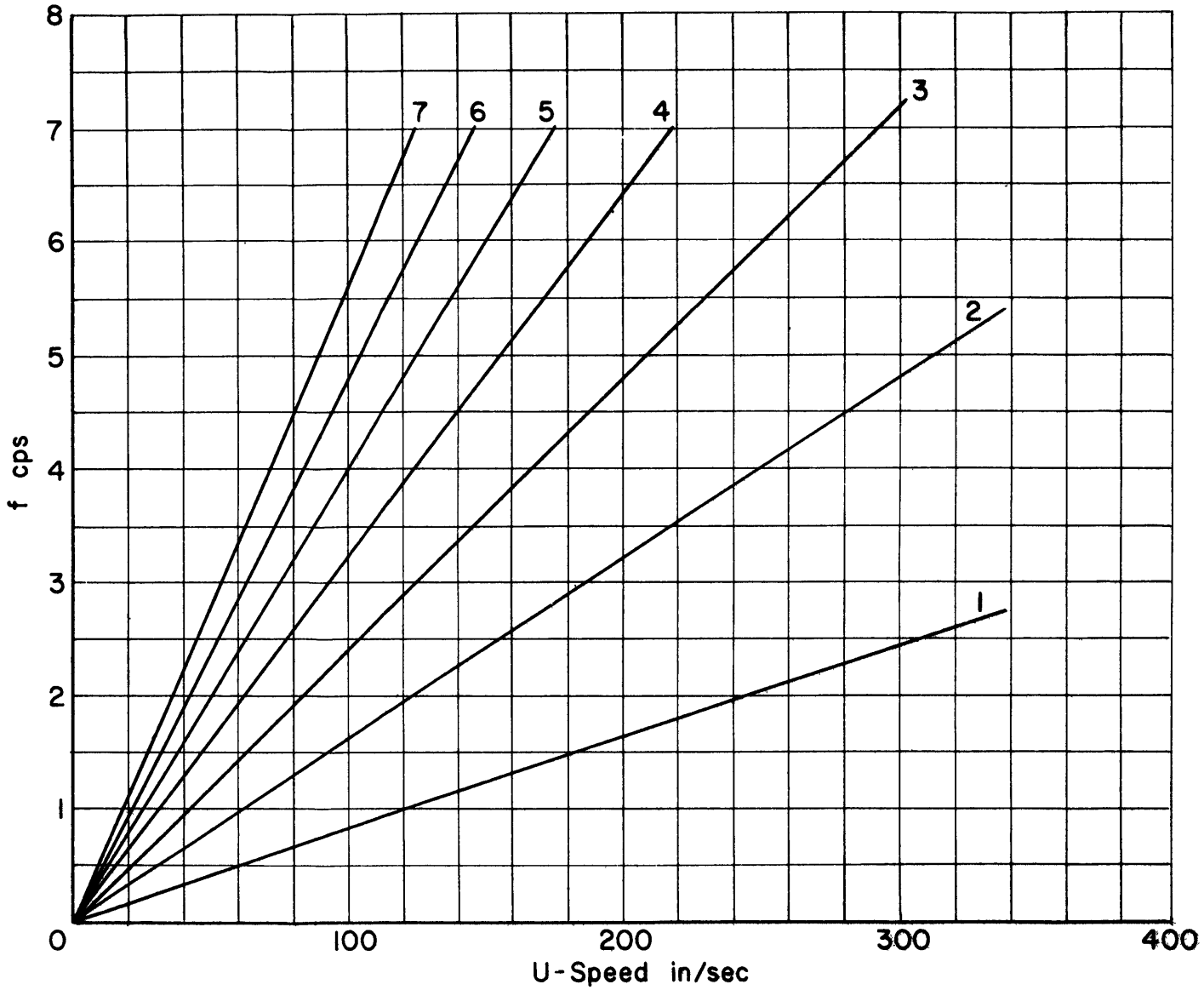

Figure 5 – Carriage Excitation Frequencies

Figure 6 – Sample Oscillatory Data

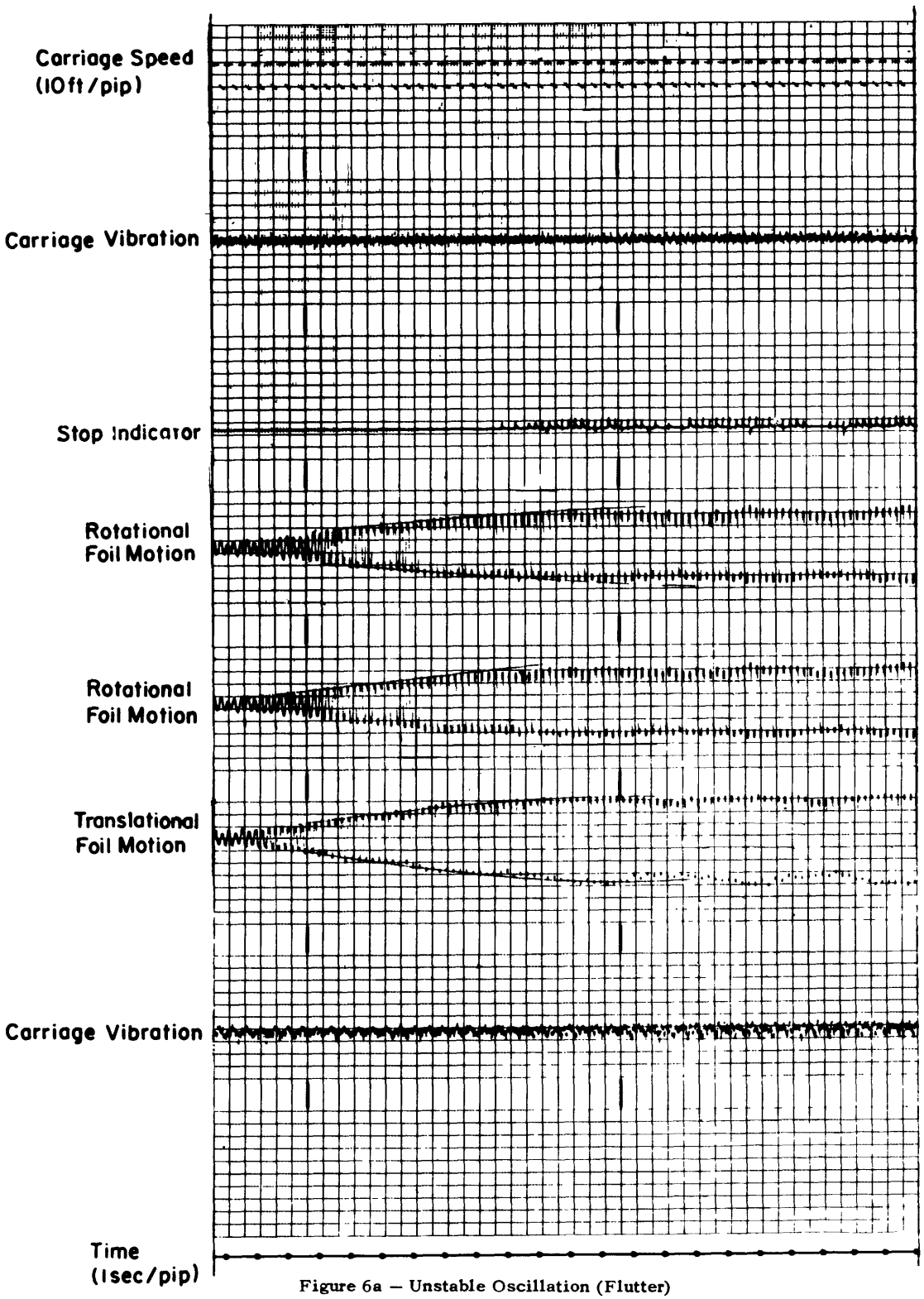

Figure 6a – Unstable Oscillation (Flutter)
Complete Record

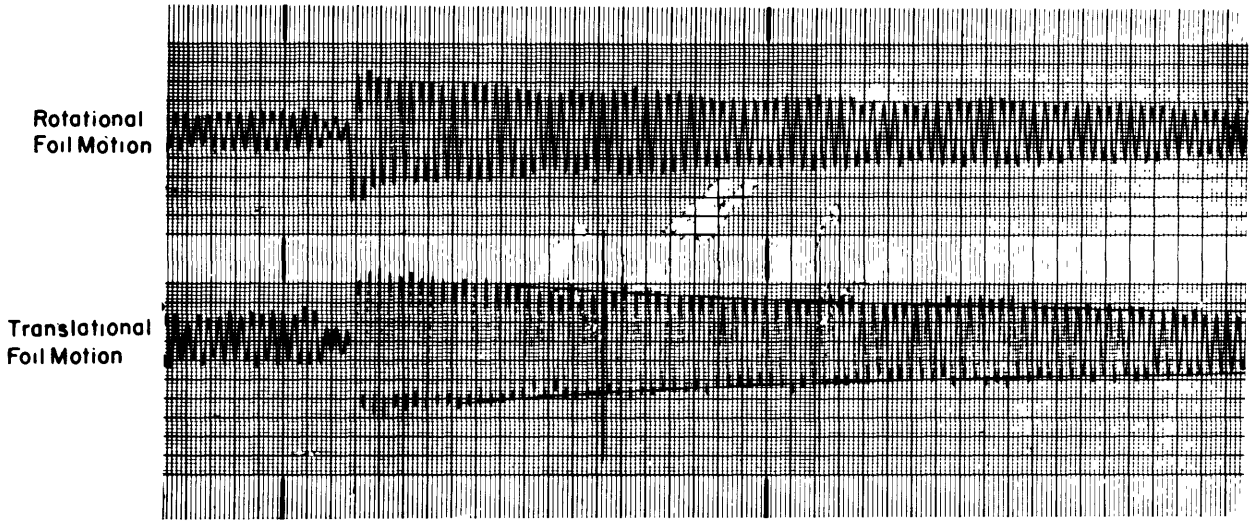

Figure 6b – Stable Oscillation

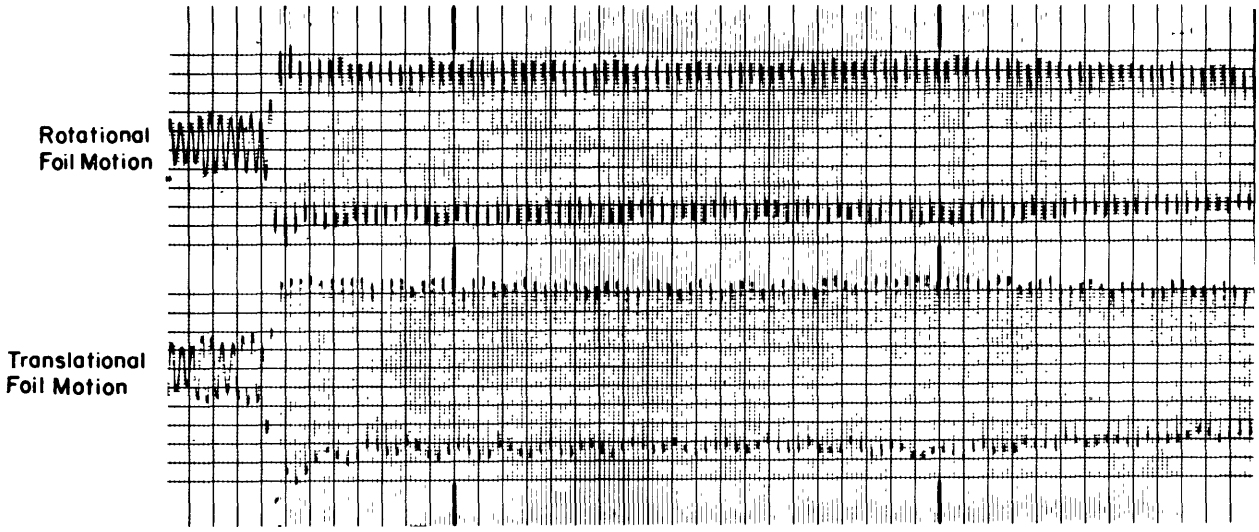

Figure 6c – Neutrally Stable Oscillation

Figure 7 – Experimental Damping Ratios and Frequencies of Vibration

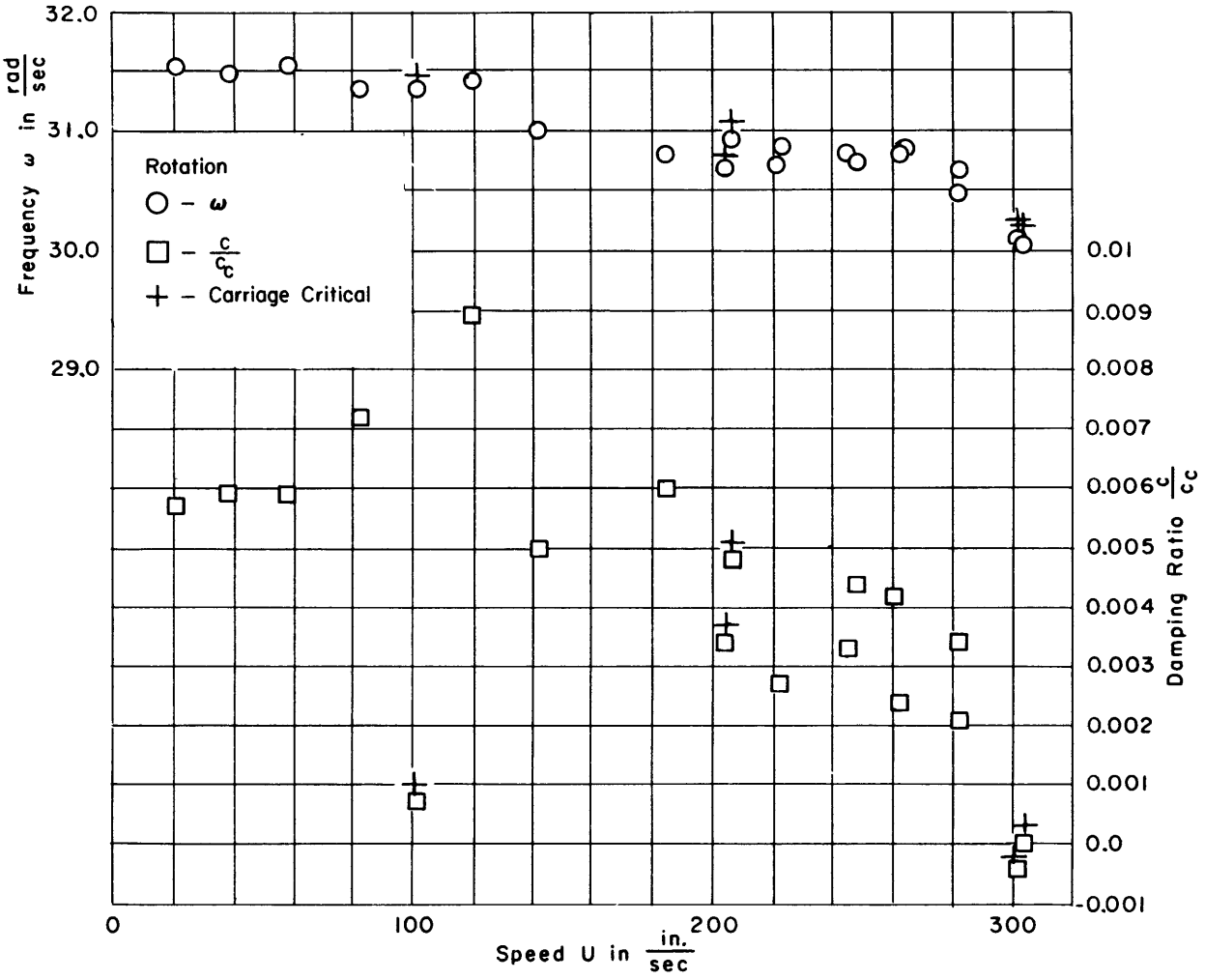

Figure 7a – Configuration A, $S_\alpha = 2.26$ lb-sec^2, Rotation

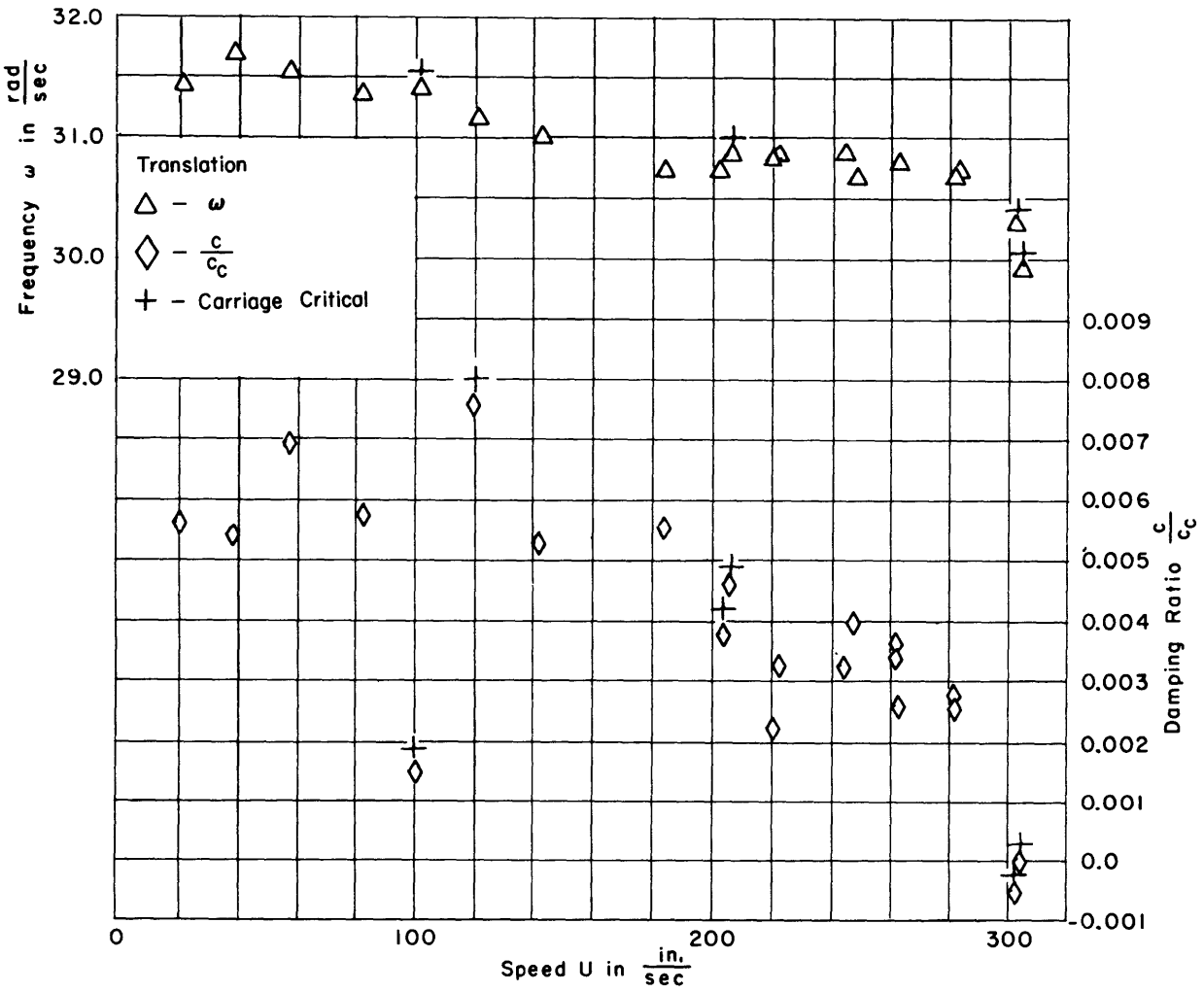

Figure 7b – Configuration A, $S_\alpha = 2.26$ lb-sec^2, Translation

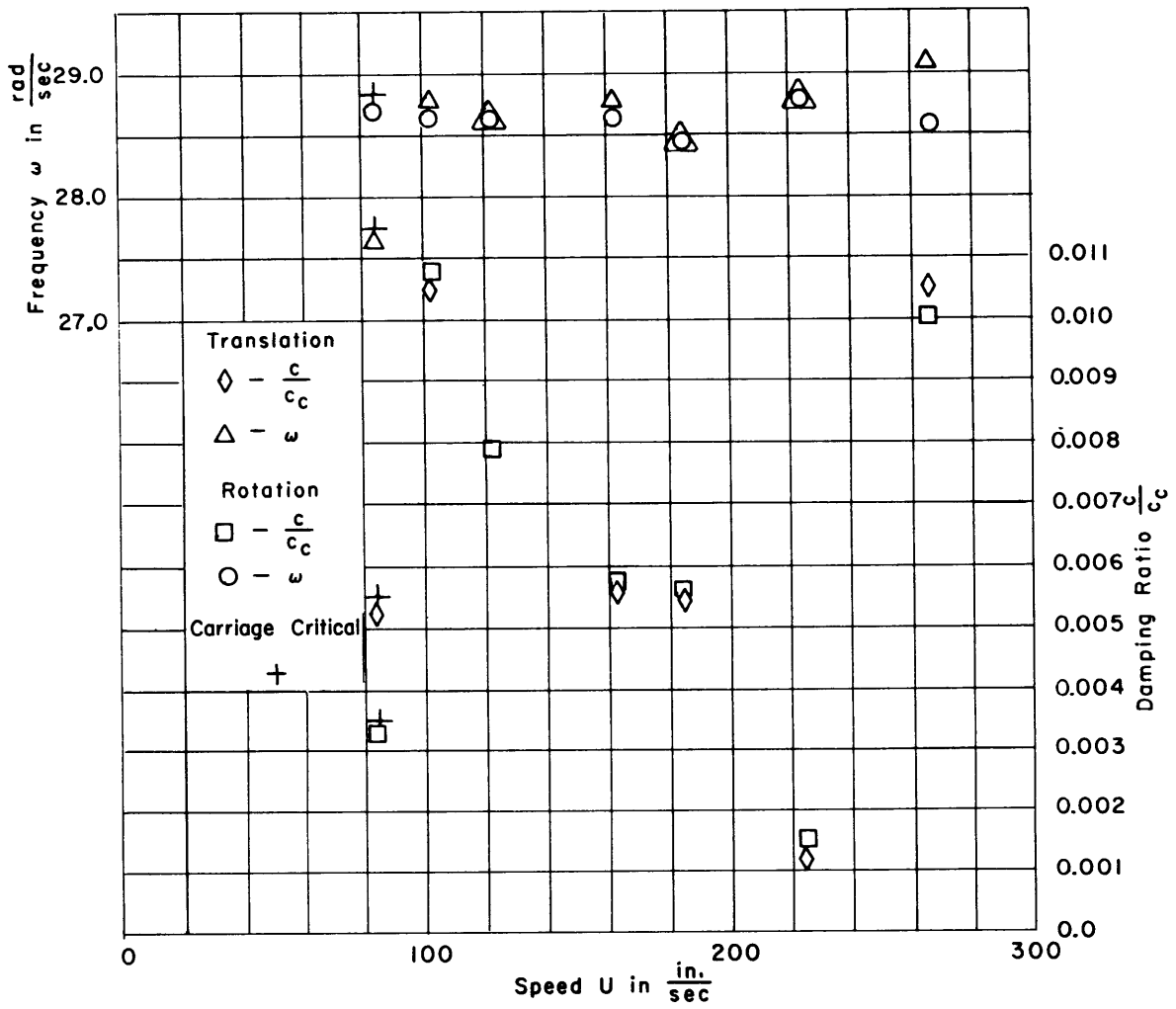

Figure 7c – Configuration B, $S_{\alpha} = 2.25$ lb-sec^2, $\alpha_s = 0.6^{\circ}$

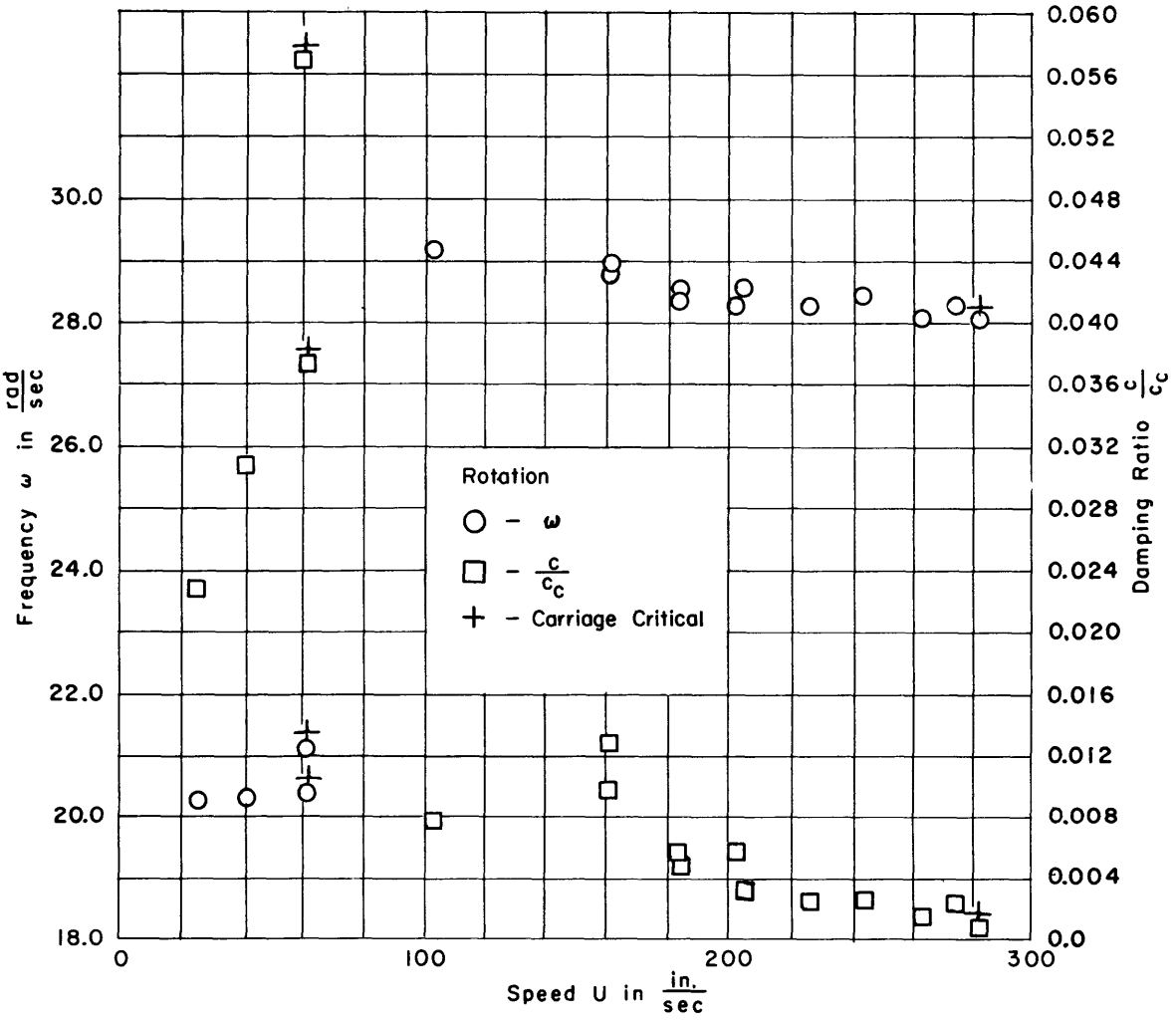

Figure 7d – Configuration, B, S_α = 2.25 lb-sec^2, Rotation

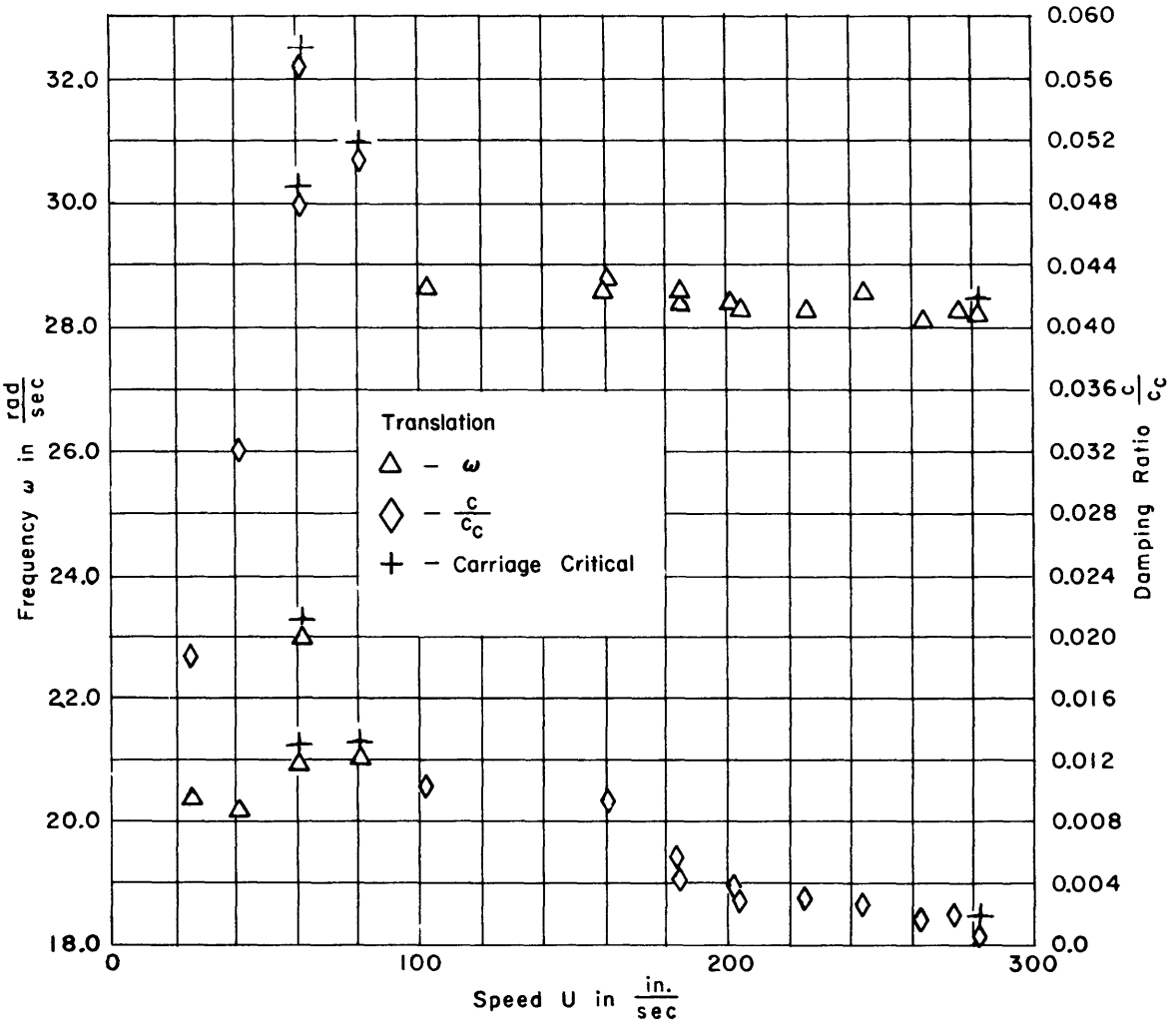

Figure 7e – Configuration B, S_α =2.25 lb-sec^2, Translation

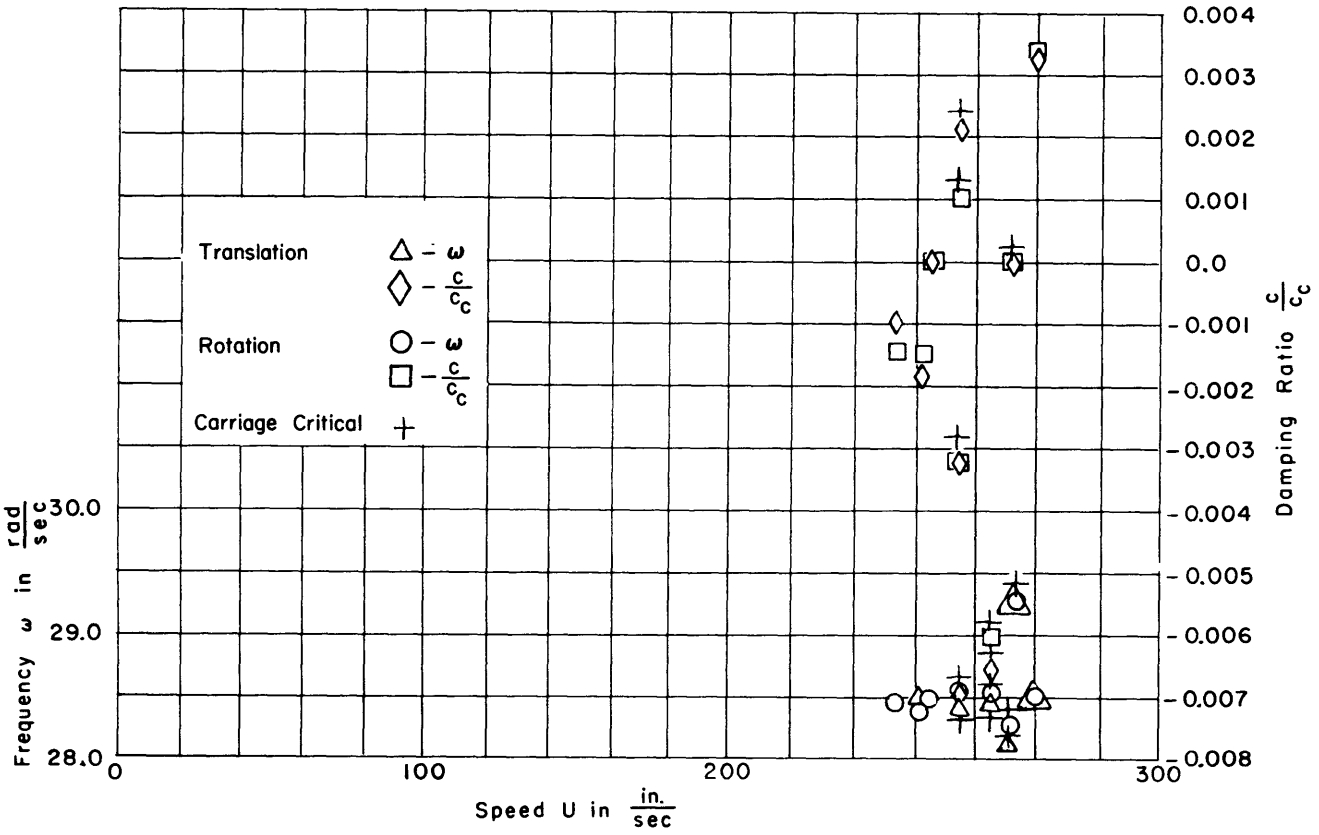

Figure 7f – Configuration B, S_α =2.49 lb-sec^2

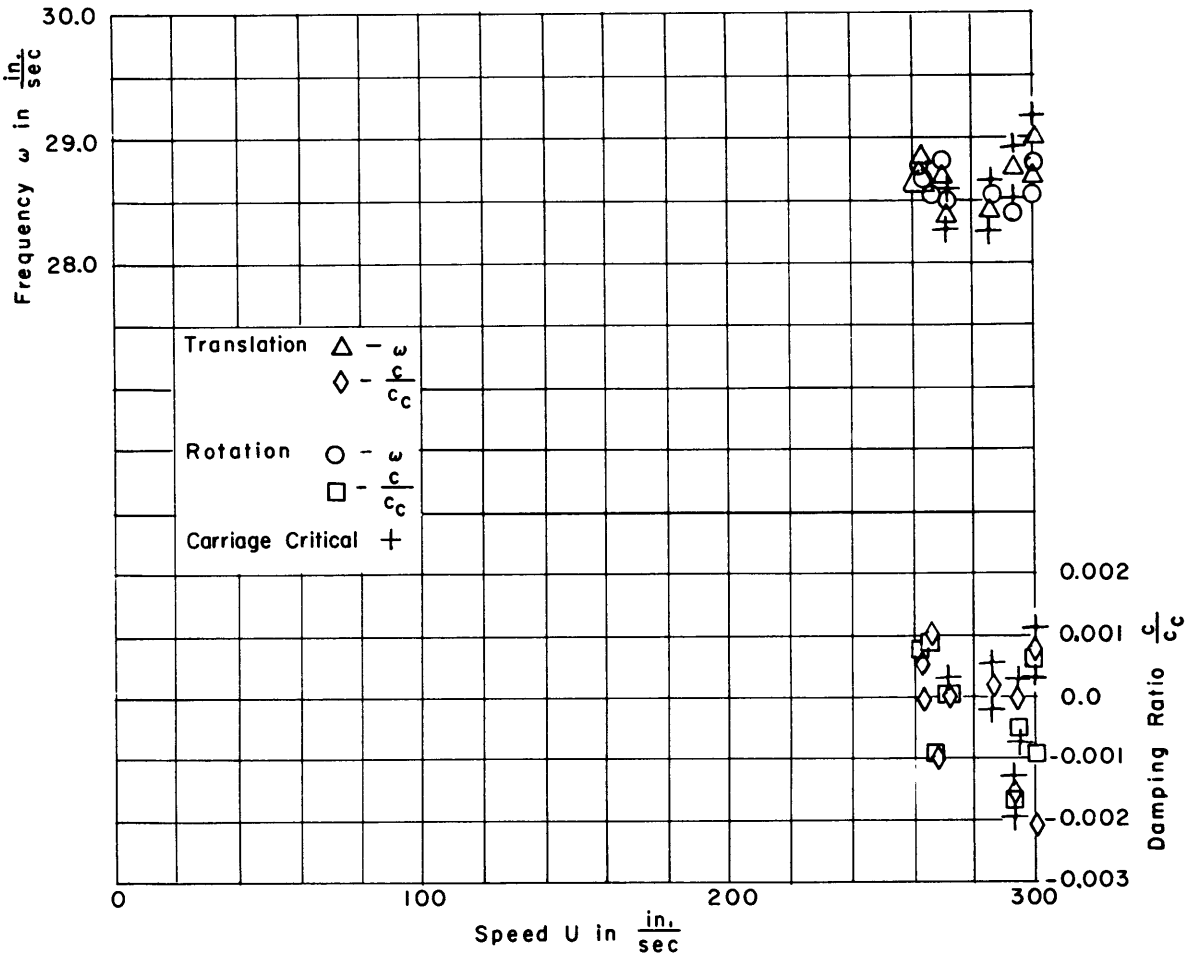

Figure 7g – Configuration B, S_{α}=2.54 lb-sec^2

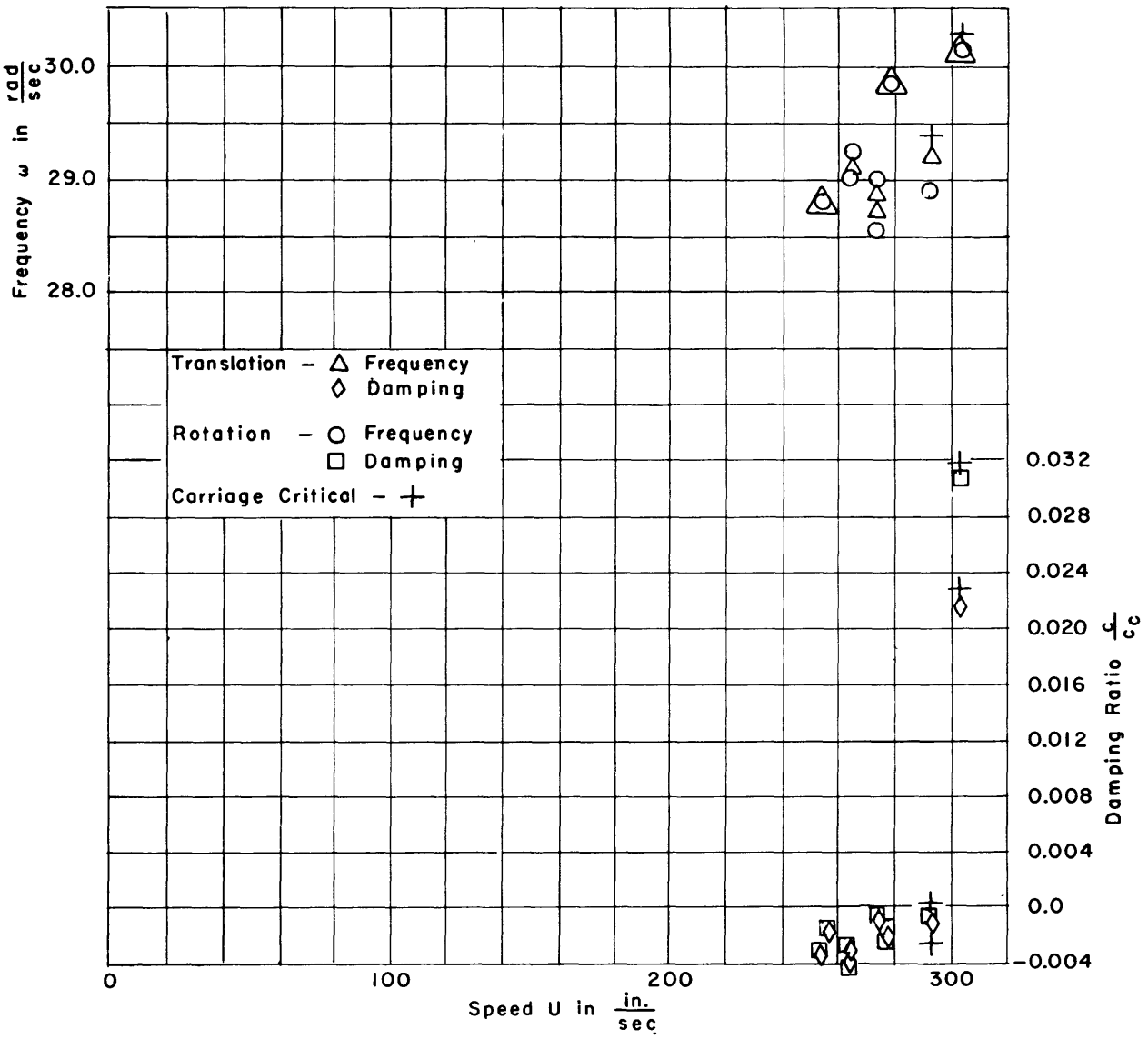

Figure 7h – Configuration B, S_α =2.66 lb-sec^2

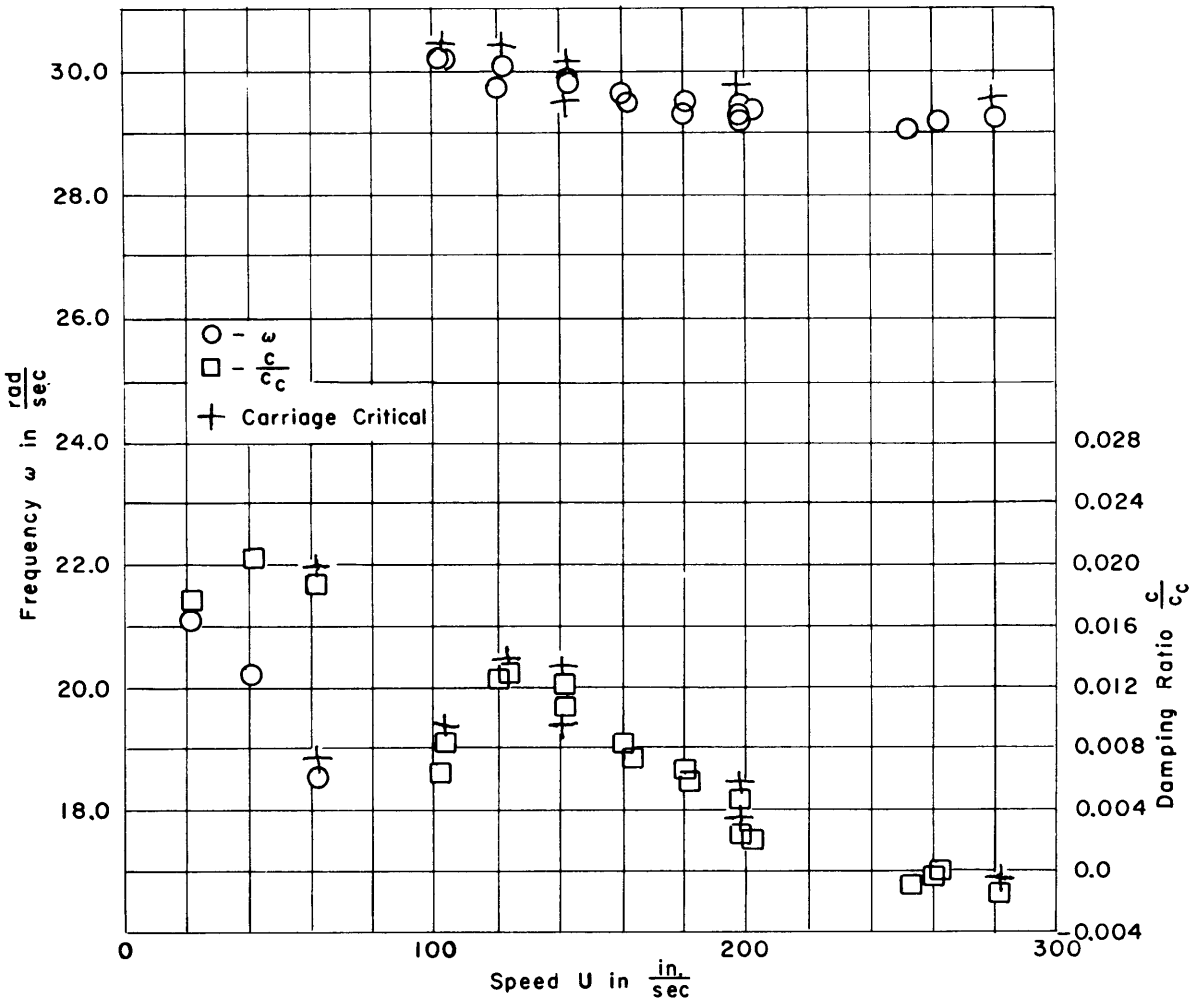

Figure 7i – Configuration B, S_{α} =2.77 lb-sec^2, Rotation

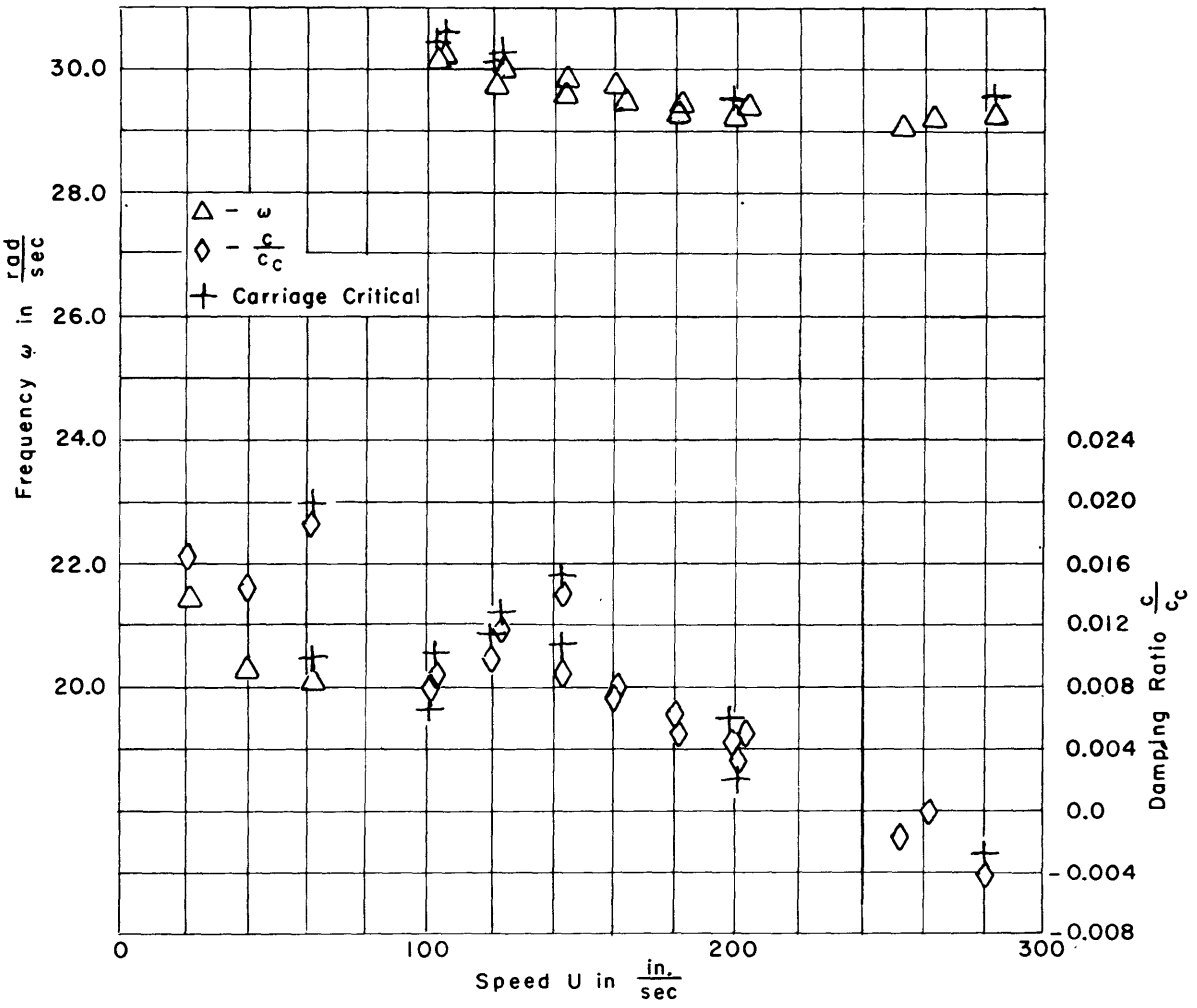

Figure 7j – Configuration B, S_α = 2.77 lb-sec^2, Translation

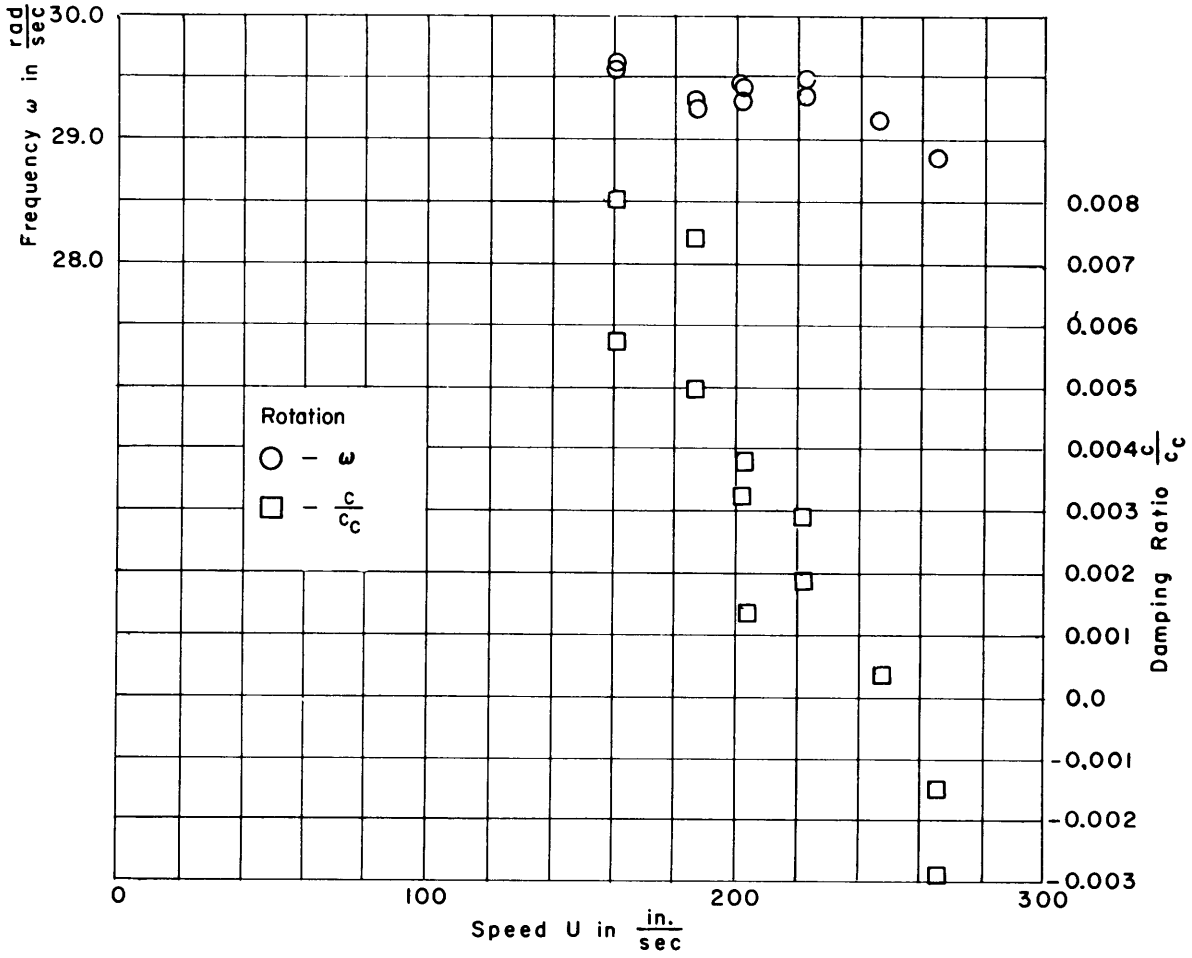

Figure 7k – Configuration B, $S_\alpha = 2.86$ lb-sec^2, Rotation

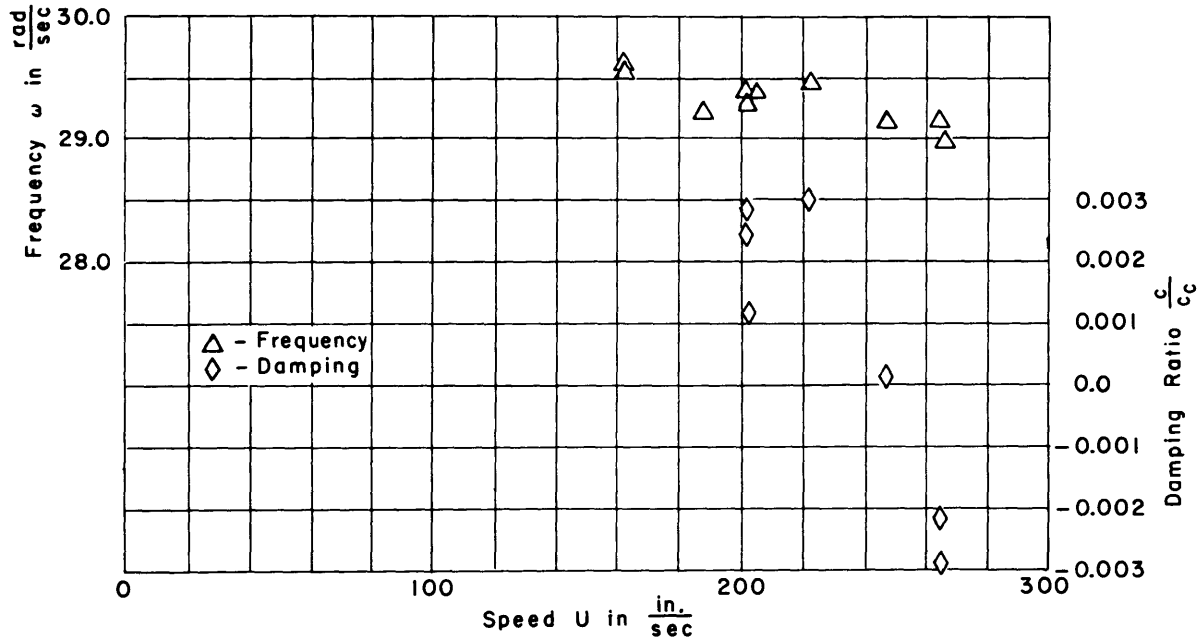

Figure 7m – Configuration B, S_α =2.86 lb-sec^2, Translation

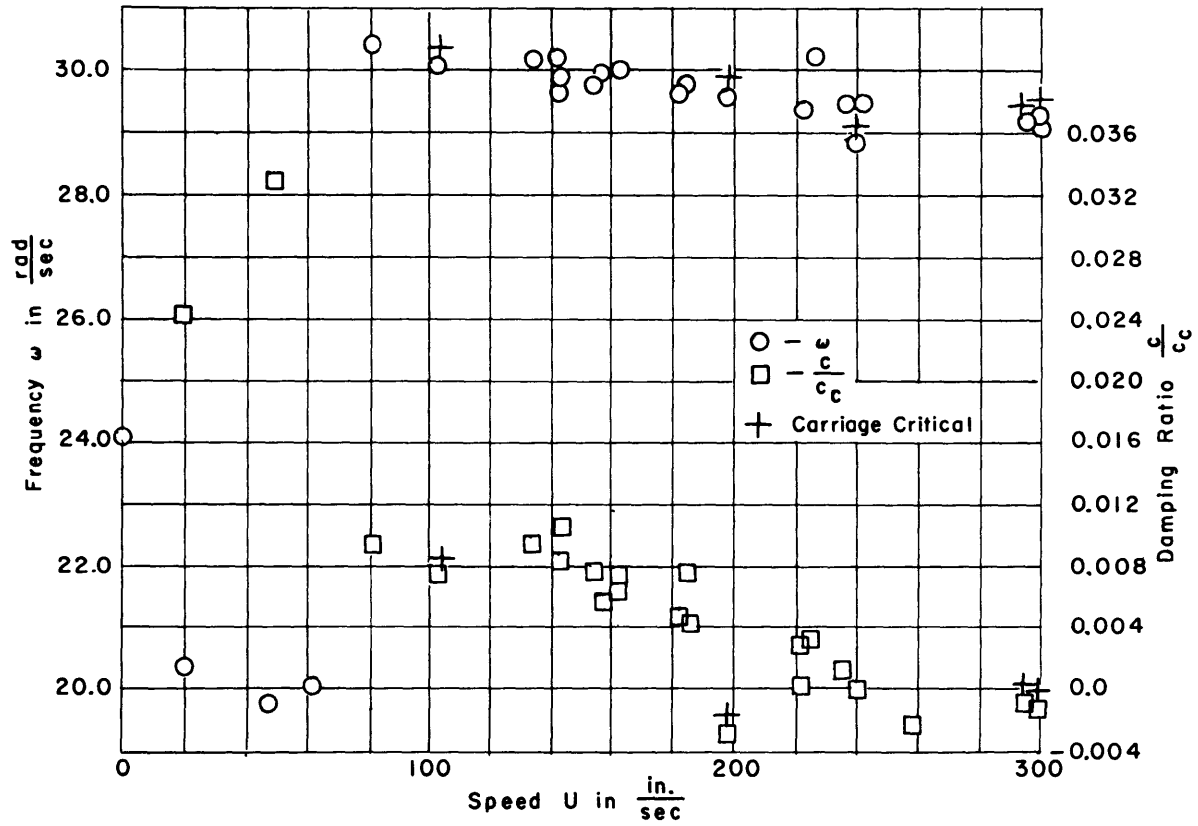

Figure 7n – Configuration B, S_α =2.93 lb-sec^2, Rotation

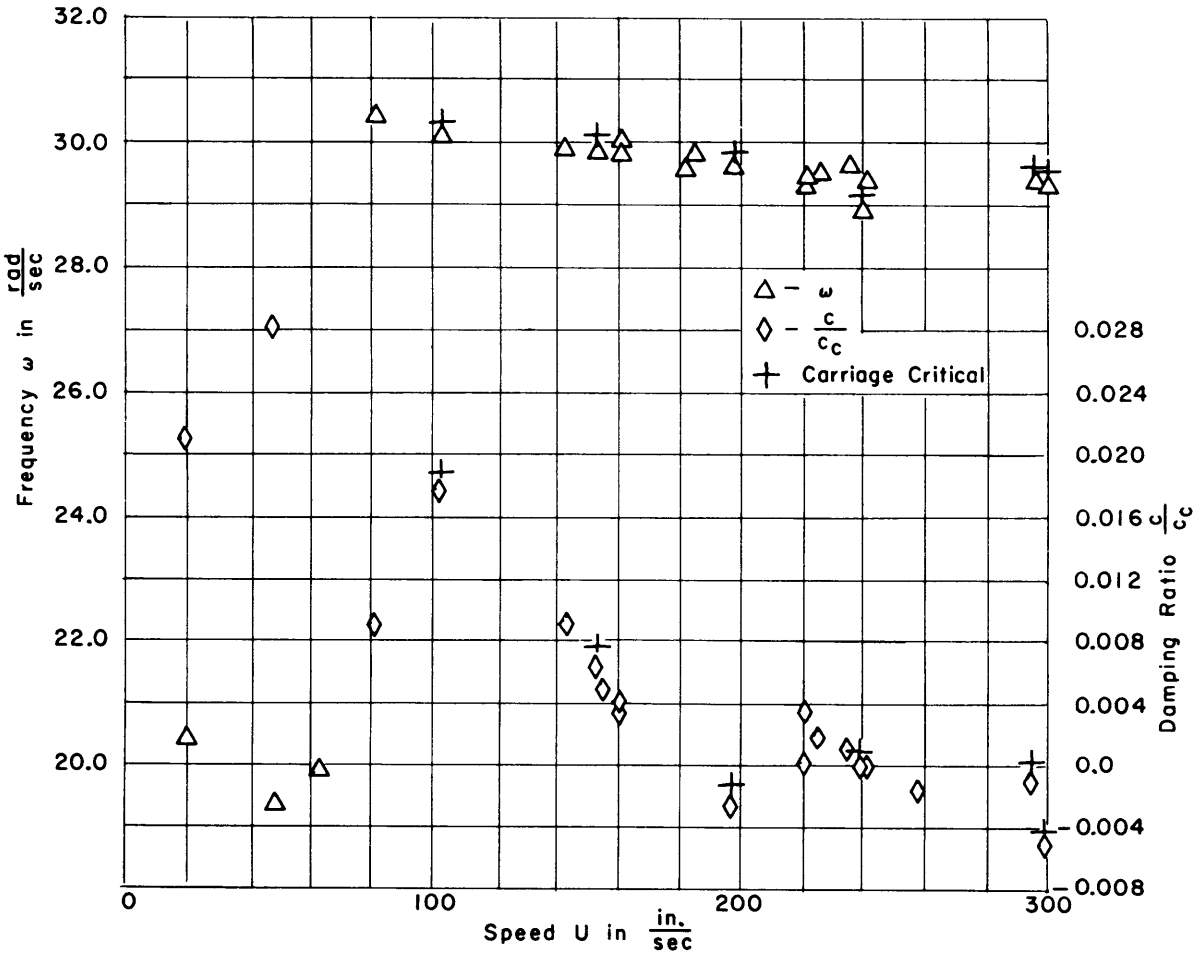

Figure 7p – Configuration B, S_{α} =2.93 lb-sec^2, Translation

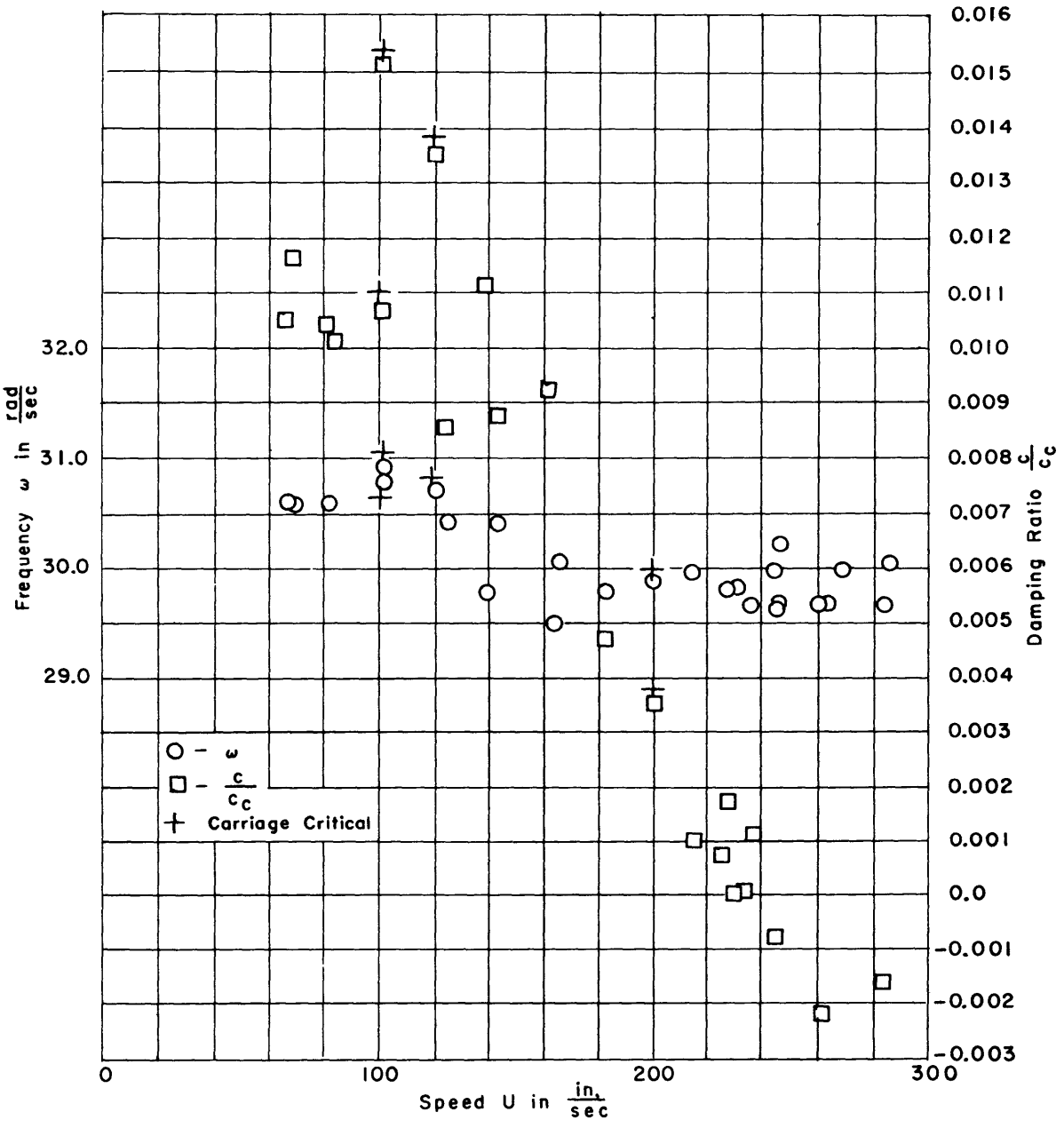

Figure 7q – Configuration B, S_α =3.94 lb-sec^2, Rotation

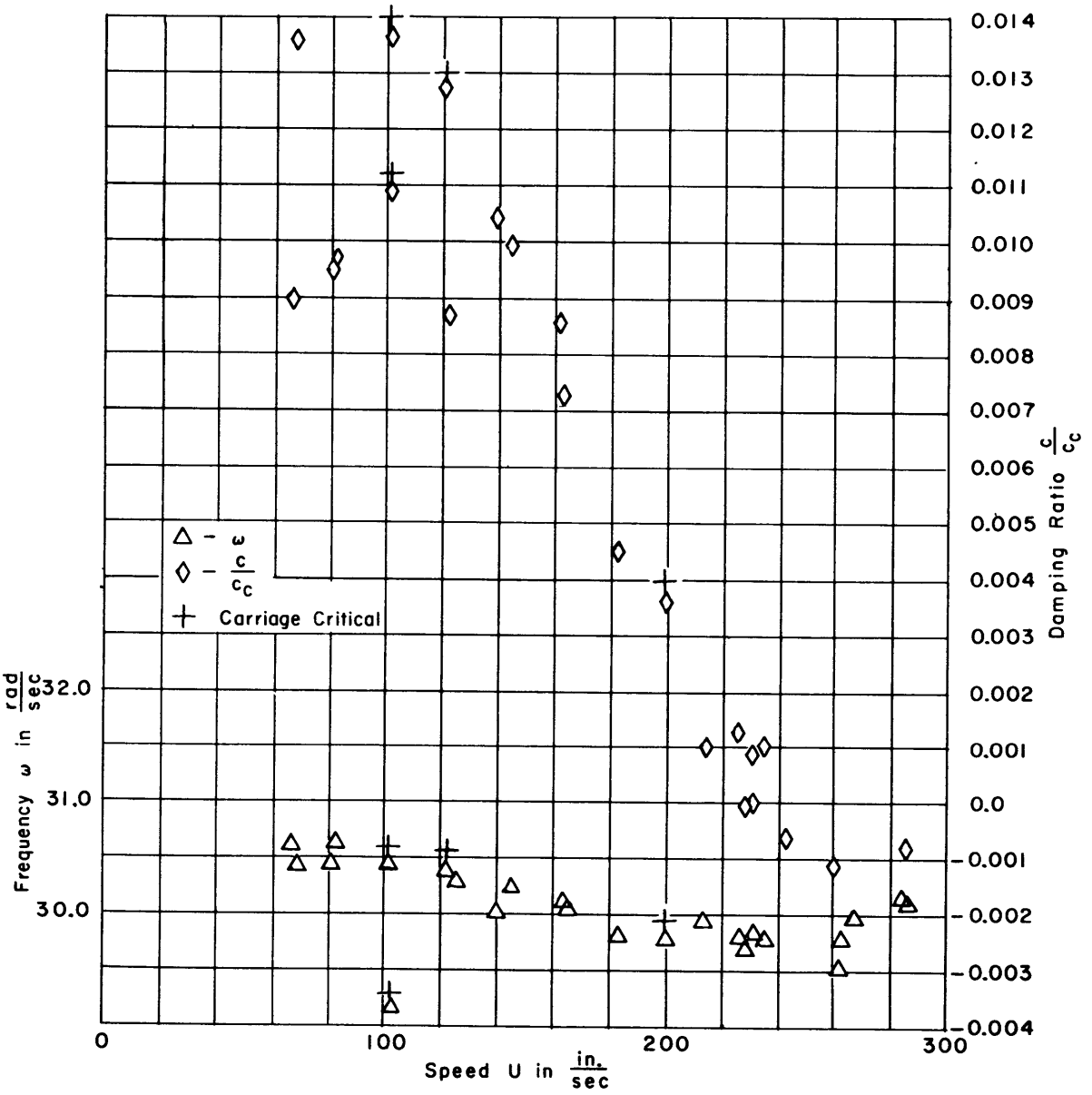

Figure 7r – Configuration B, S_{α} =3.04 lb-sec^2, Translation

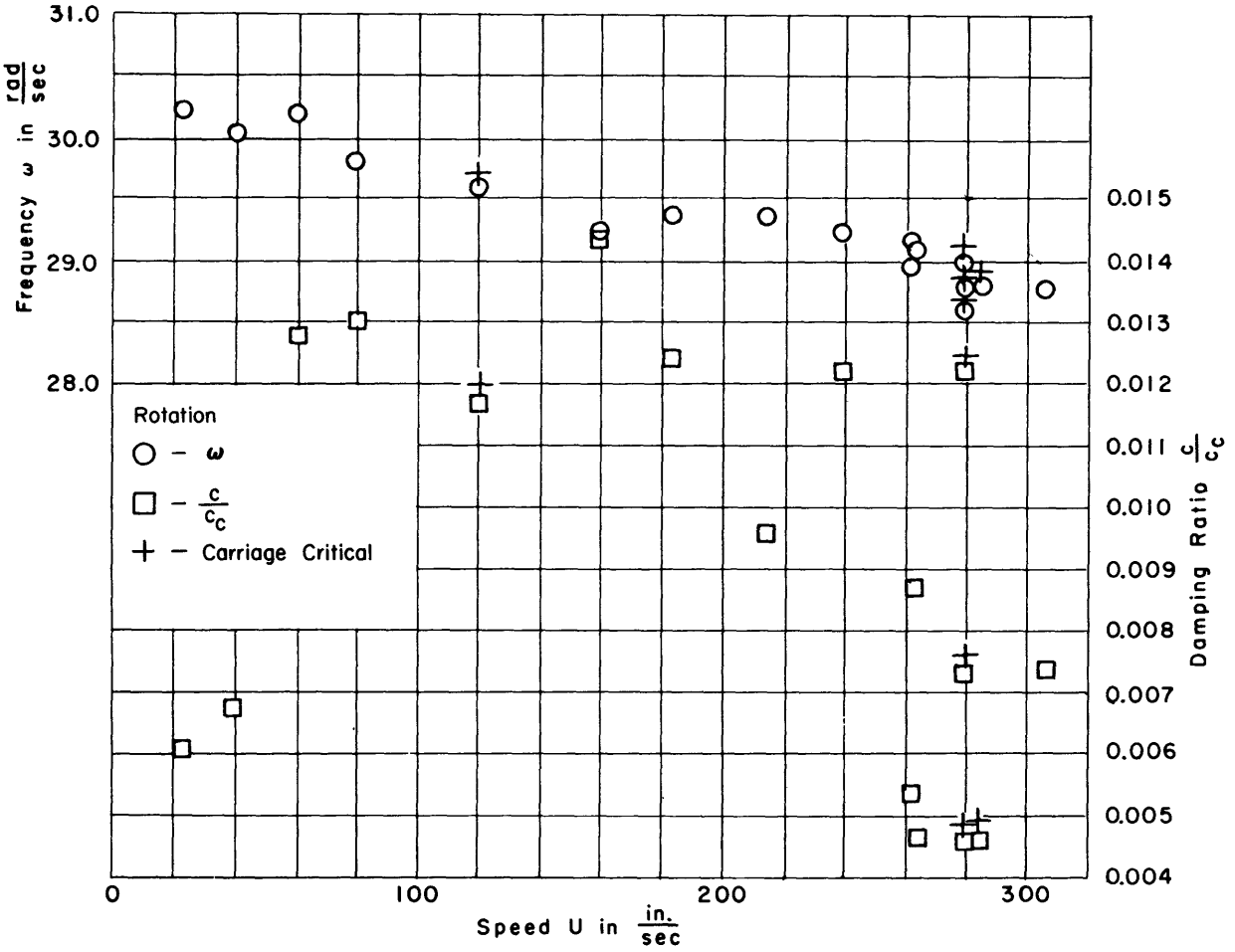

Figure 7s – Configuration C, $S_\alpha = 2.26$ lb-sec^2, Rotation

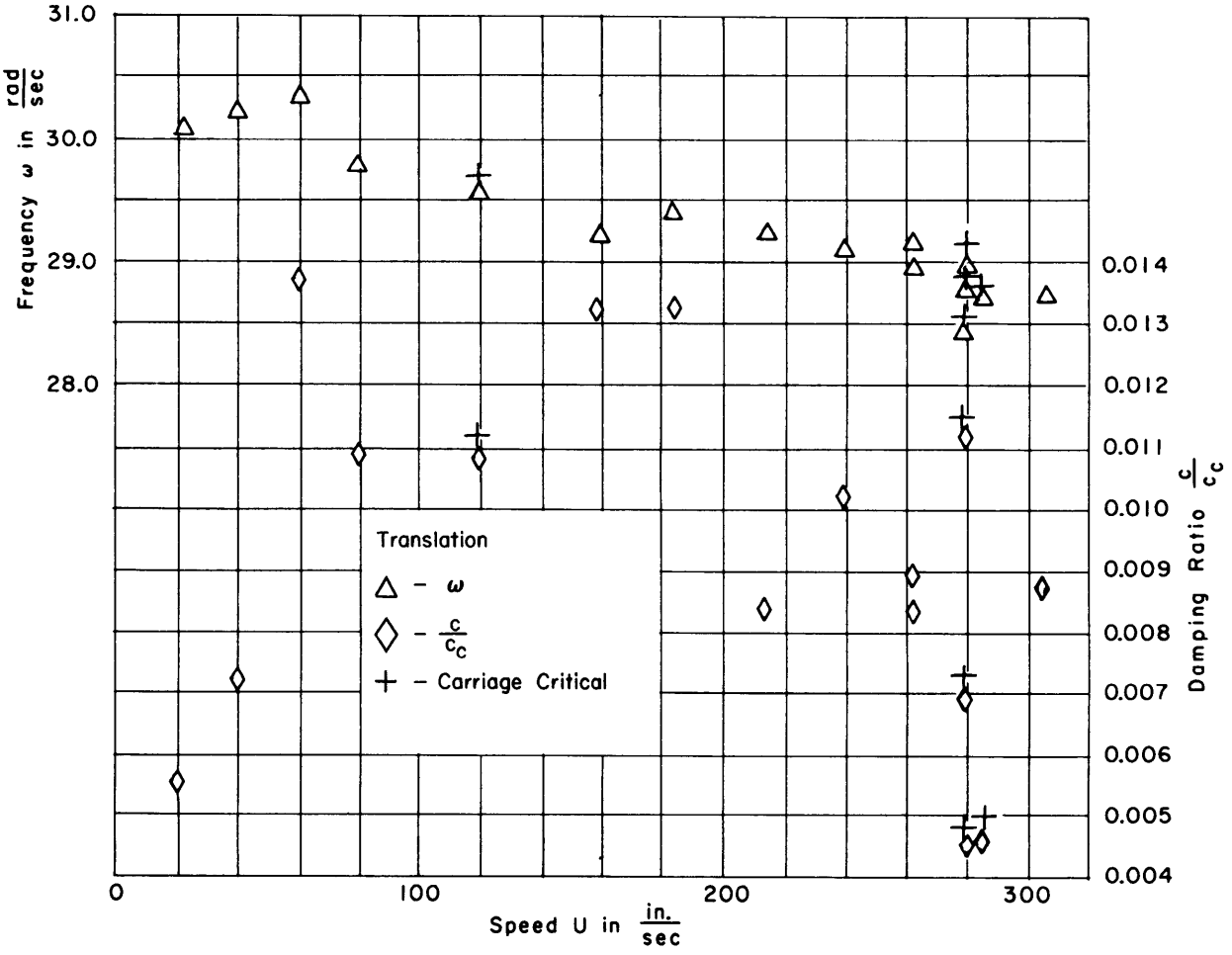

Figure 7t – Configuration C, S_α=2.26 lb-sec^2, Translation

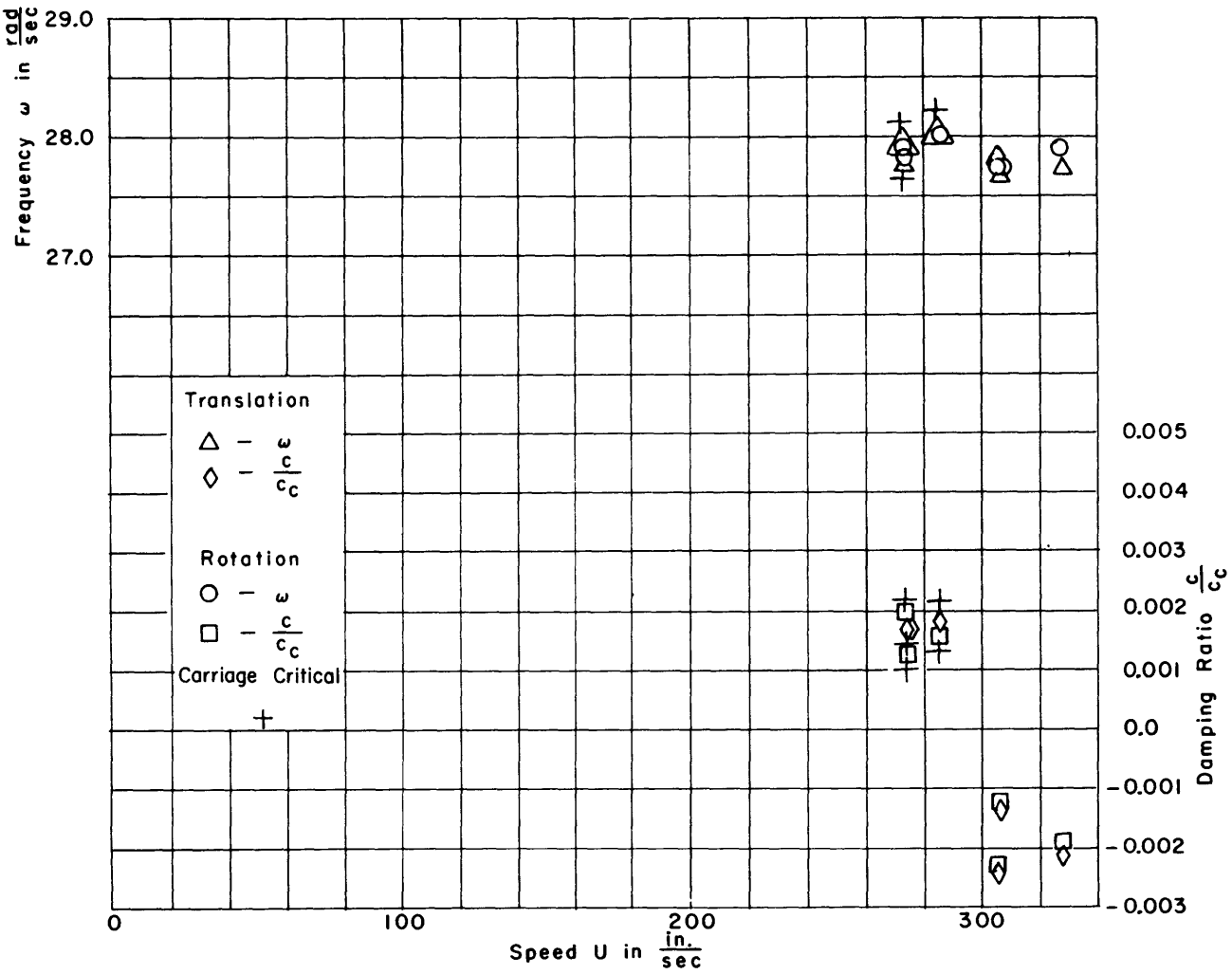

Figure 7u – Configuration D, S_α =2.77 lb-sec^2

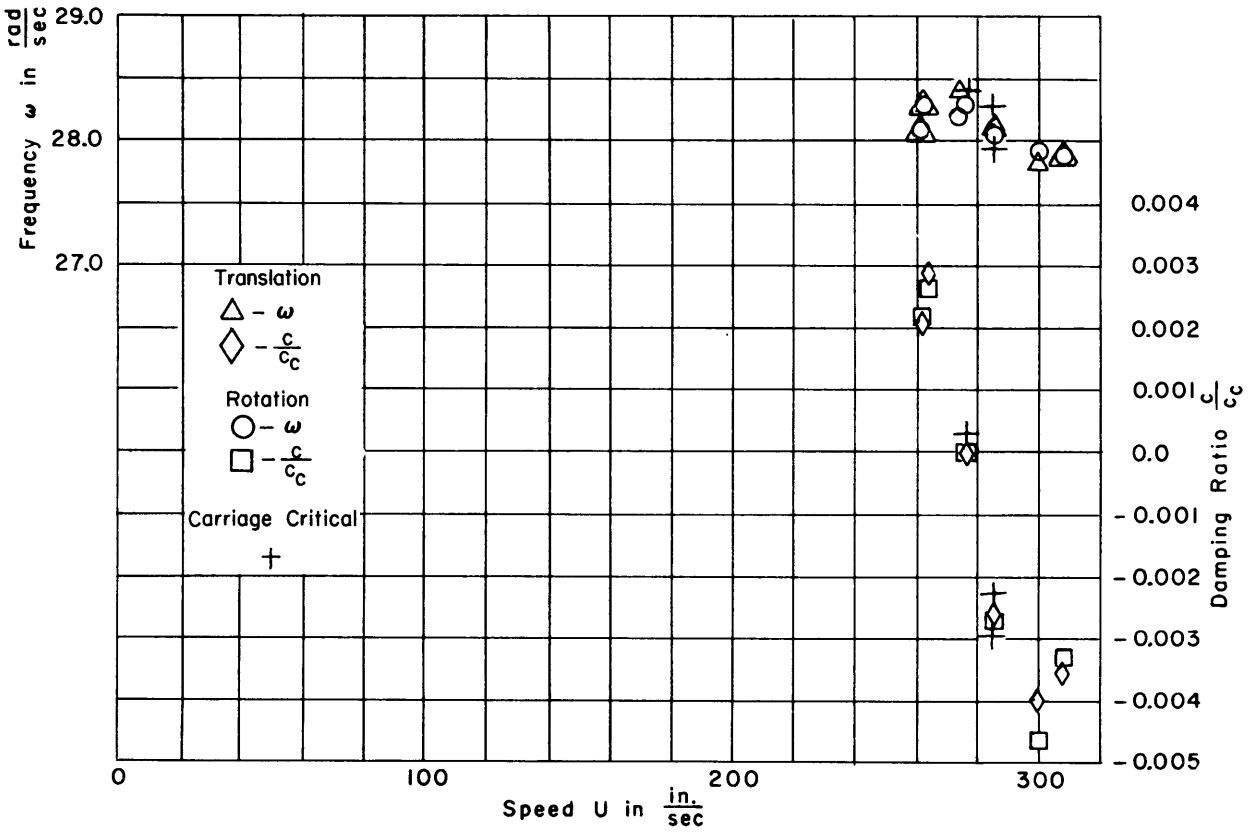

Figure 7v – Configuration D, S_{α}=2.93 lb-sec^2

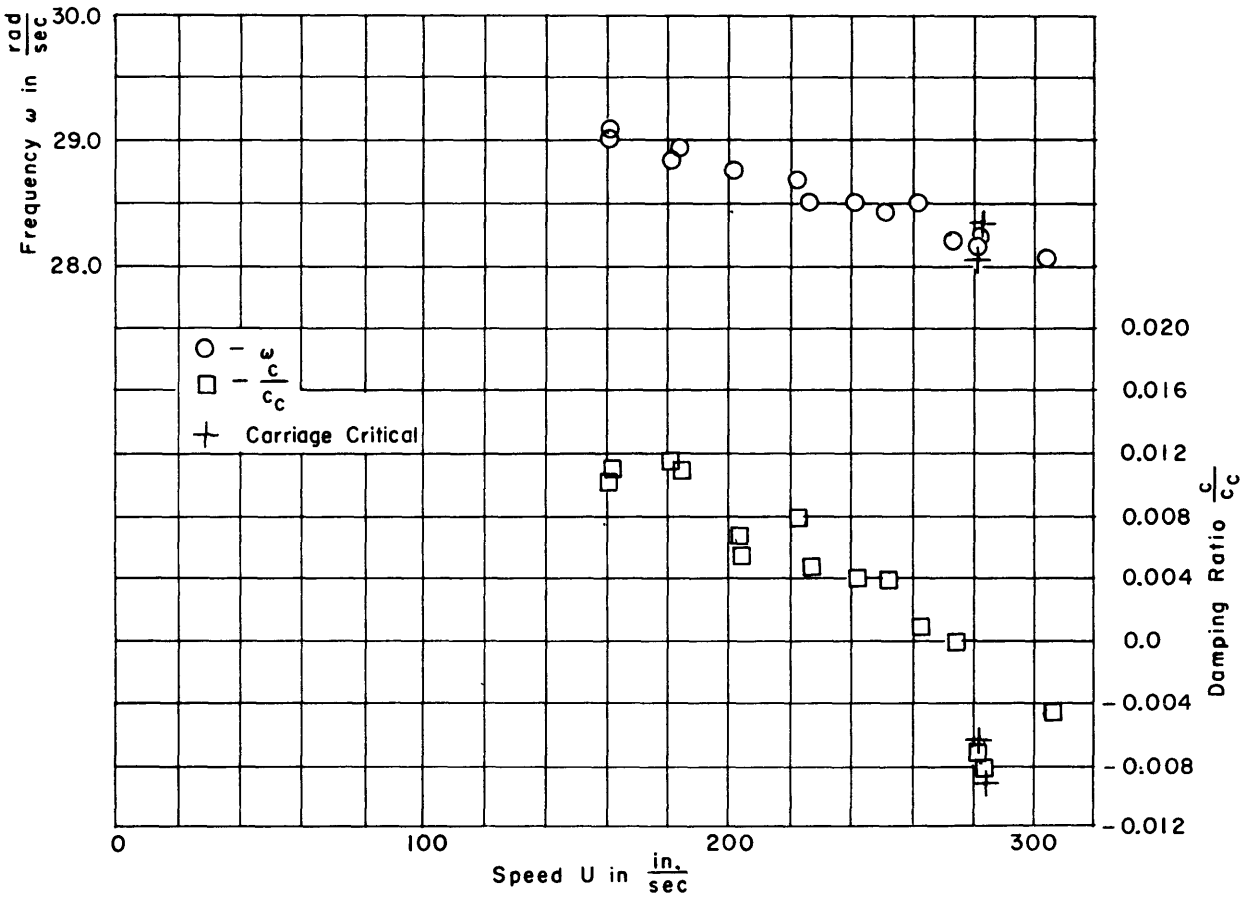

Figure 7w – Configuration D, S_α=3.04 lb-sec^2, Rotation

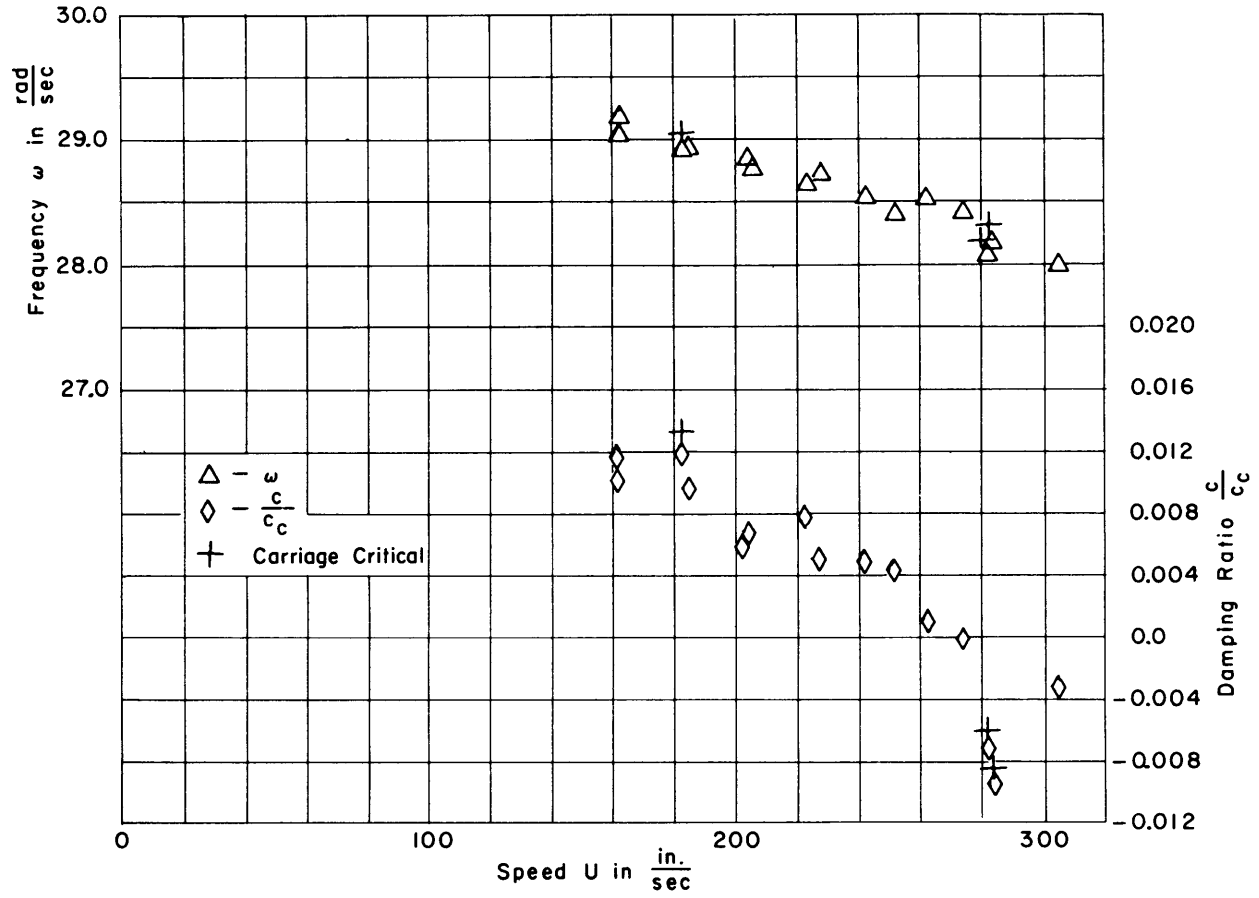

Figure 7x – Configuration D, S_{α}=3.04 lb-sec^2, Translation

Figure 8 – Theoretical Damping and Frequency Data

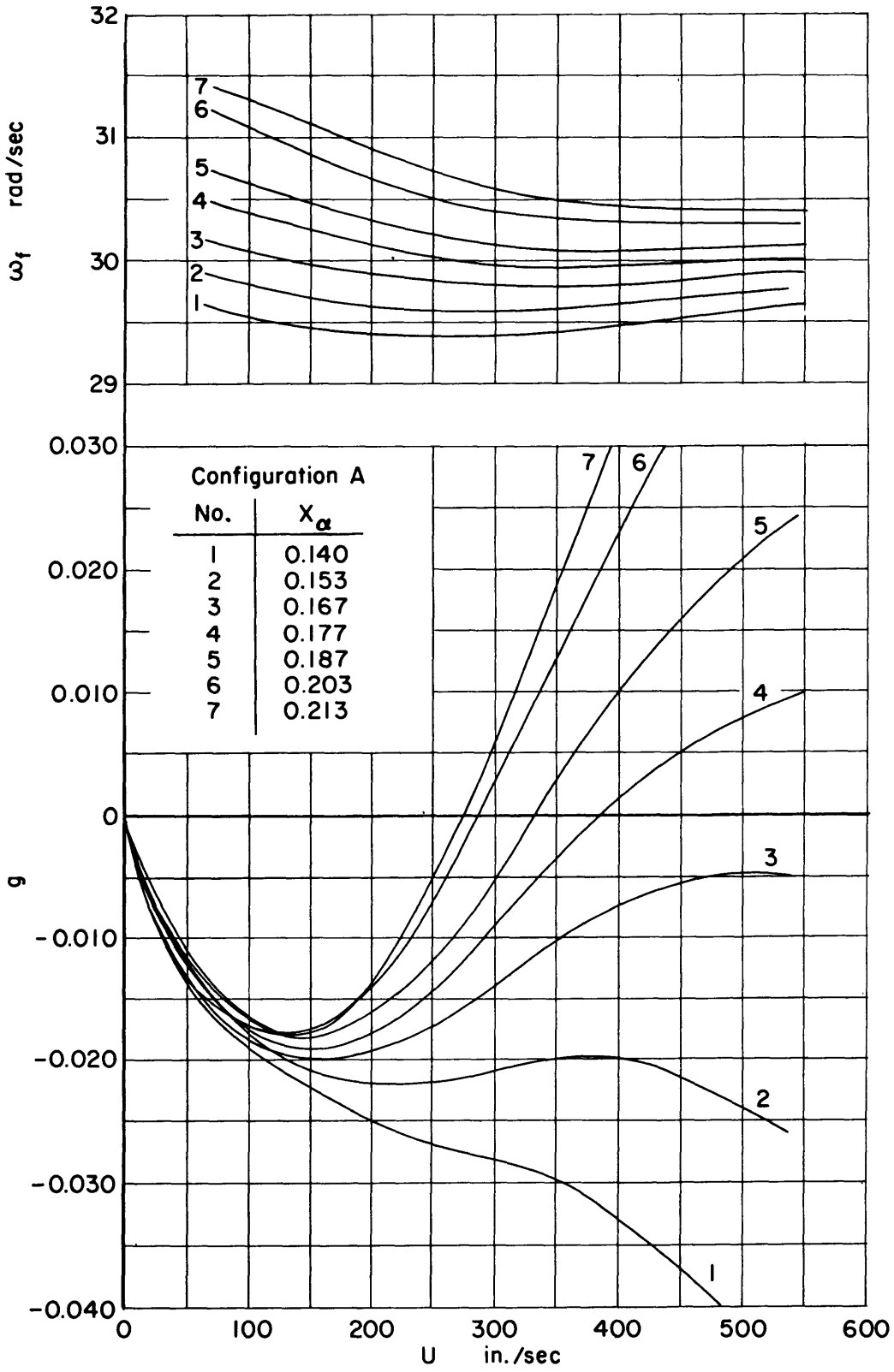

Figure 8a

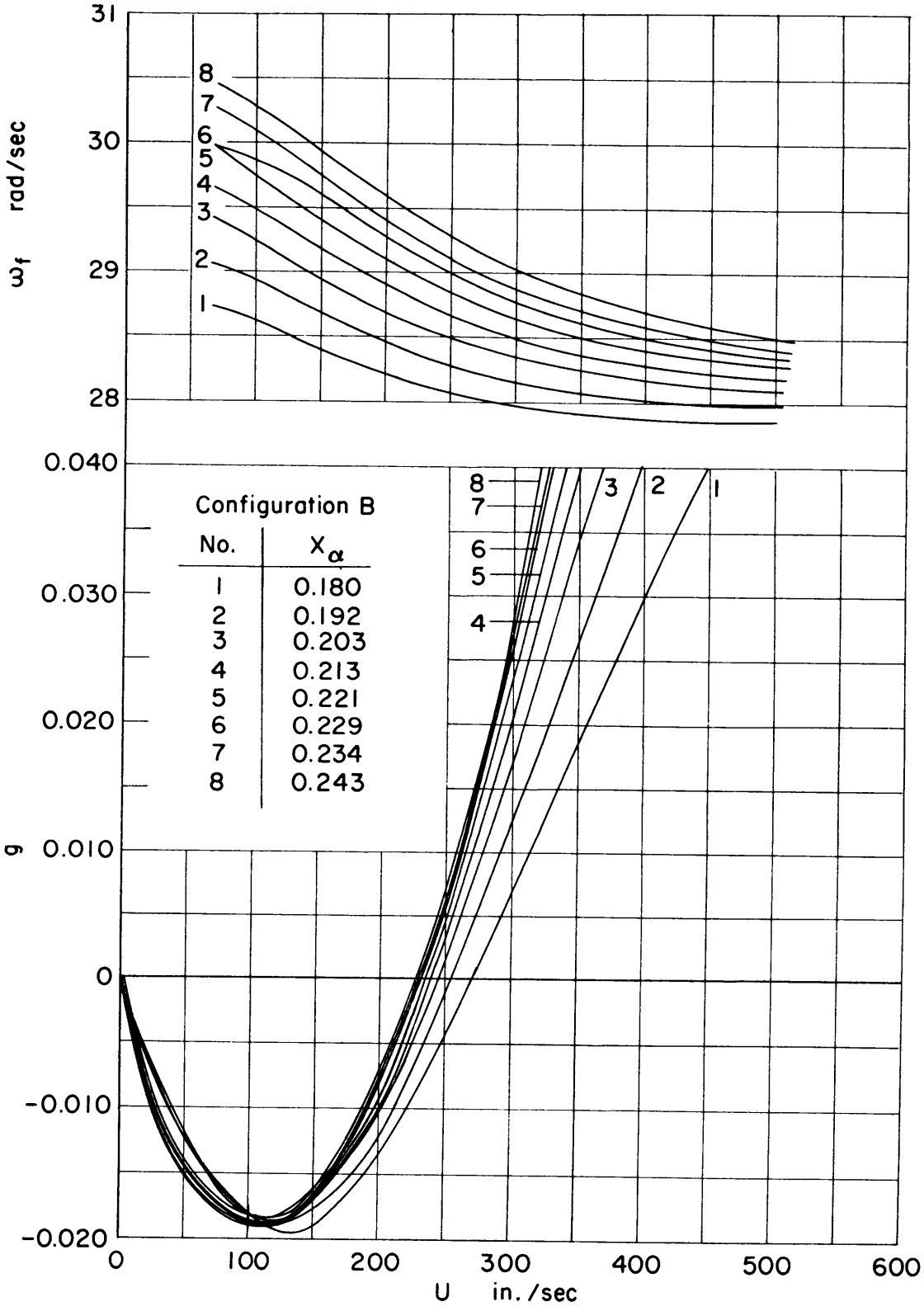
31
30
29
28
ω_f rad/sec
8
7
6
5
4
3
2
1
0.040
0.030
0.020
0.010
0
-0.010
-0.020
g
Configuration B
No. | X_α
1 0.180
2 0.192
3 0.203
4 0.213
5 0.221
6 0.229
7 0.234
8 0.243
0
100
200
300
400
500
600
U in./sec

Figure 8b

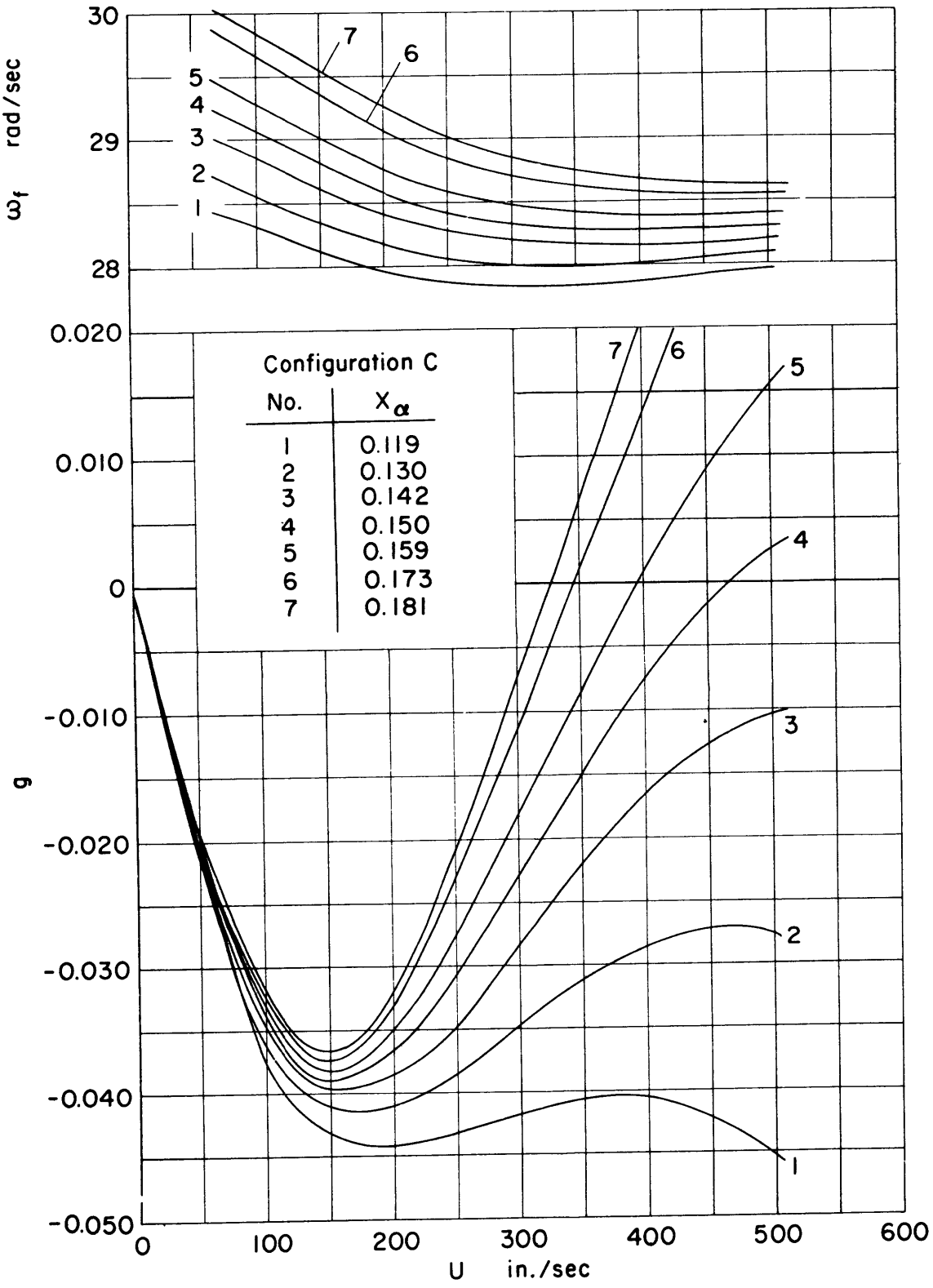
30
29
28
ω_f rad/sec
7
6
5
4
3
2
1
0.020
0.010
0
-0.010
-0.020
-0.030
-0.040
-0.050
g
Configuration C
No. | X_α
1 0.119
2 0.130
3 0.142
4 0.150
5 0.159
6 0.173
7 0.181
0
100
200
300
400
500
600
U in./sec

Figure 8c

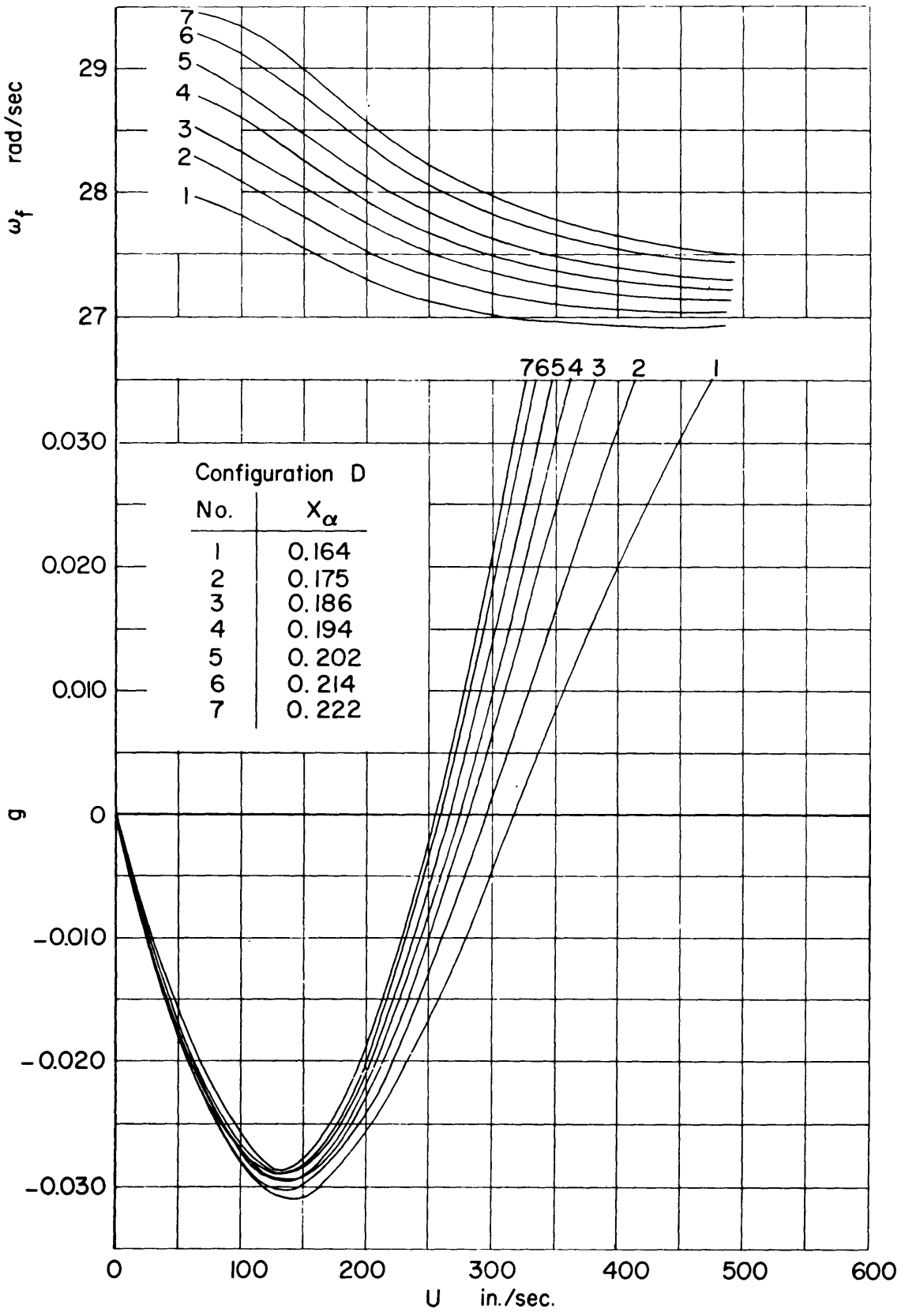
7
6
5
4
3
2
1
29
28
27
ω_f rad/sec
7 6 5 4 3 2 1
0.030
0.020
0.010
0
-0.010
-0.020
-0.030
g
Configuration D
No. | X_α
1 | 0.164
2 | 0.175
3 | 0.186
4 | 0.194
5 | 0.202
6 | 0.214
7 | 0.222
0
100
200
300
400
500
600
U in./sec.

Figure 8d

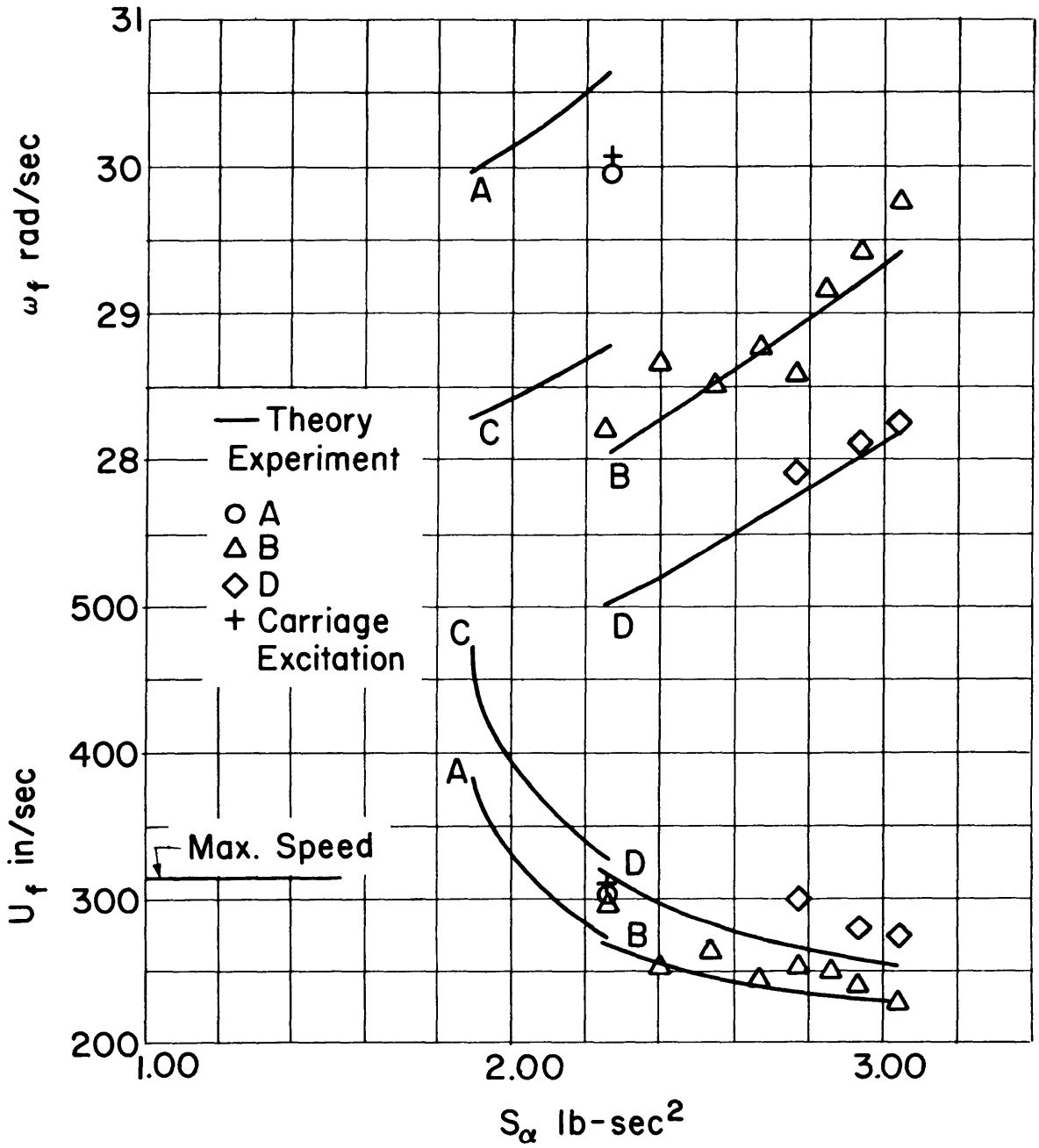

Figure 9 – Critical Speeds and Frequencies

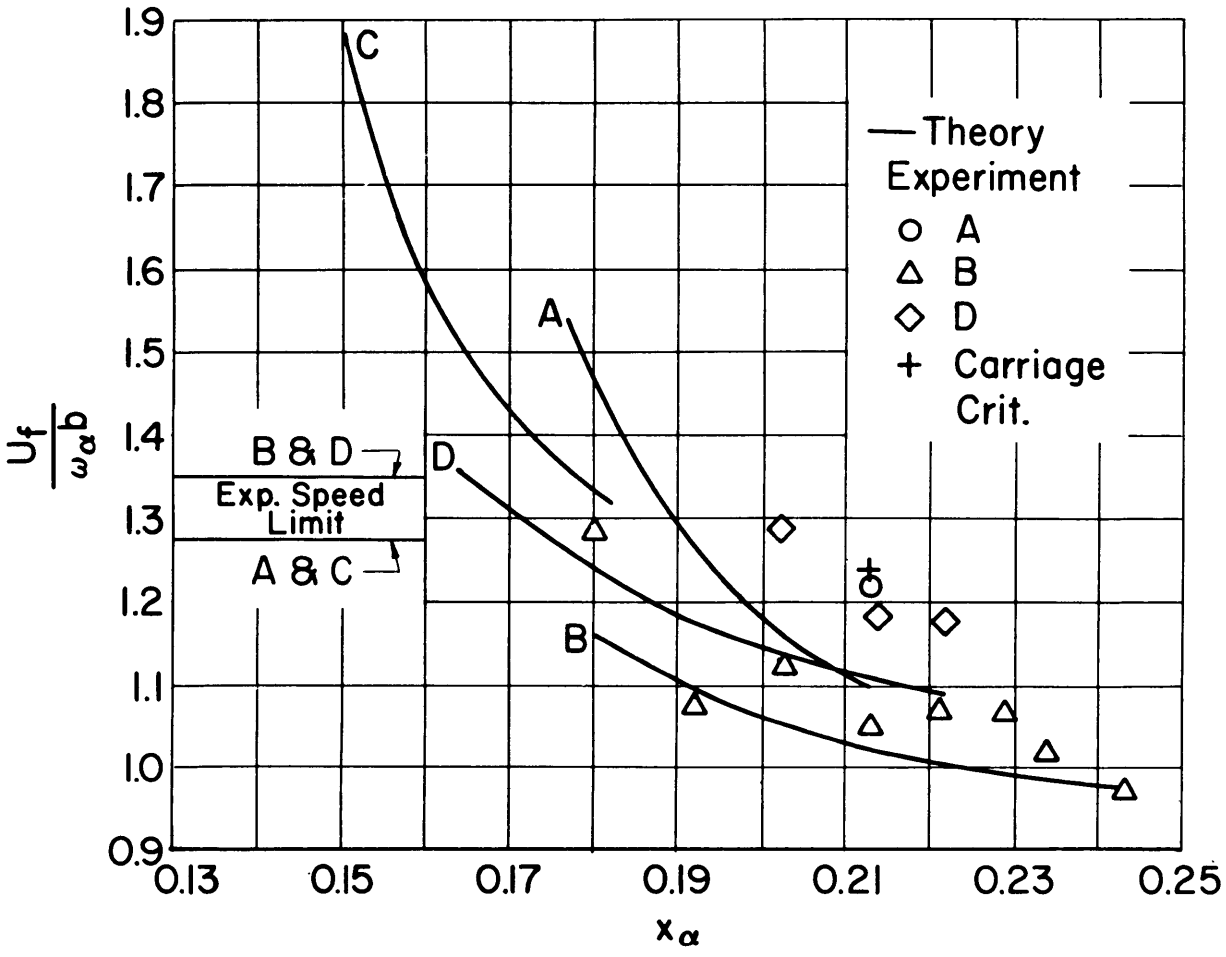

Figure 10 – Dimensionless Critical Flutter Parameters

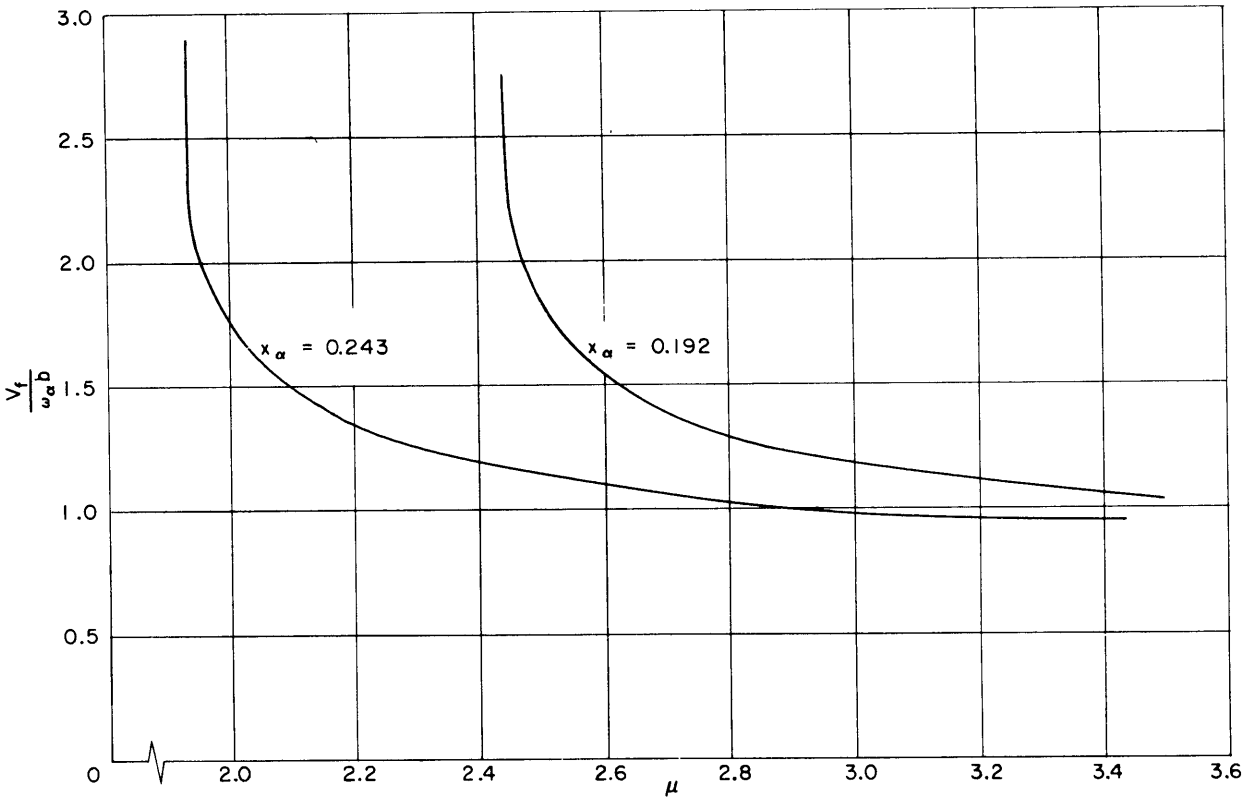

Figure 11 – Theoretical Critical Speed Dependence on Mass-Density Ratio

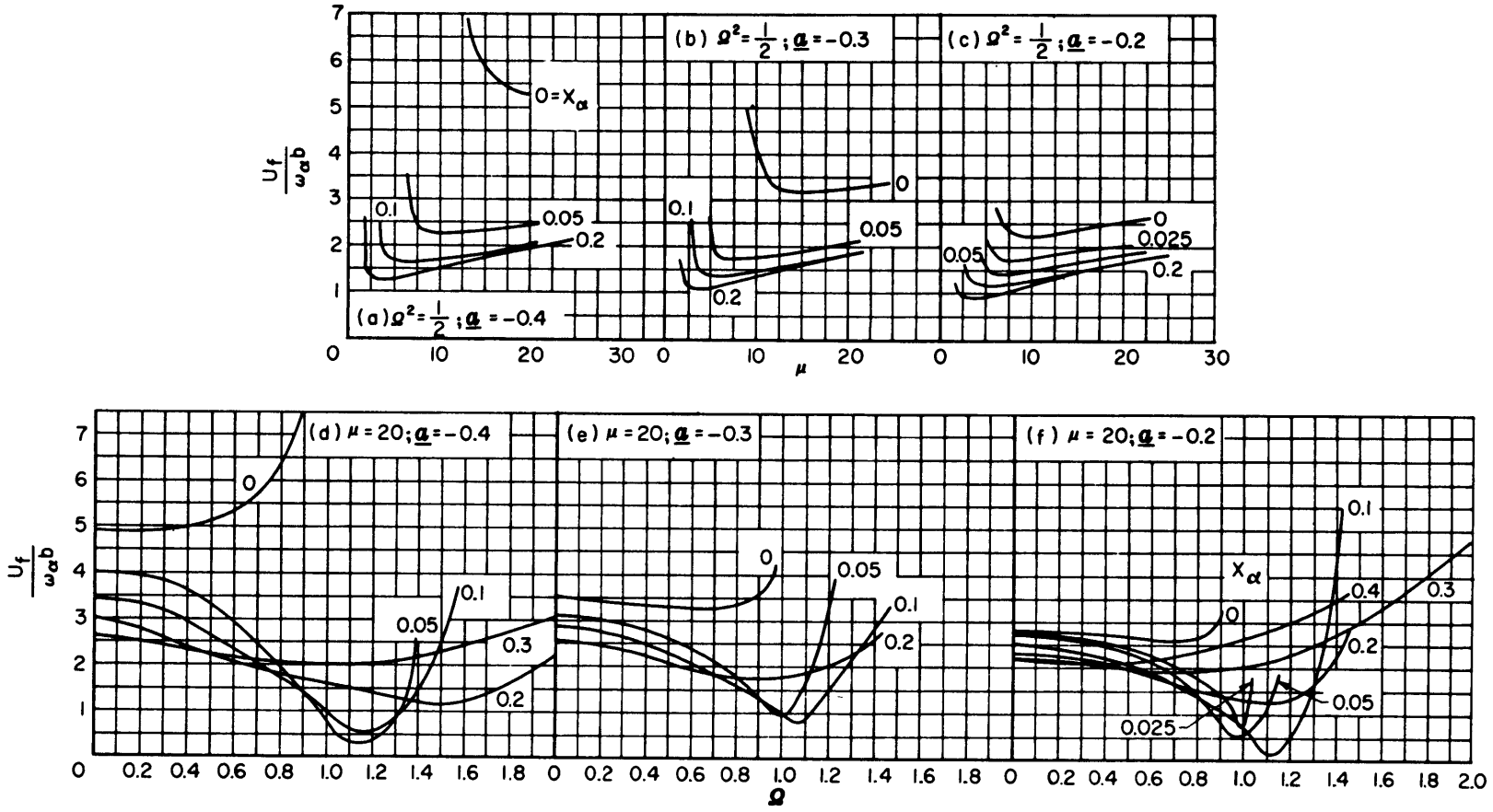

Figure 12 – Theoretical Critical Flutter Speeds

INITIAL DISTRIBUTION

Copies

8 CHBUSHIPS
- 3 Tech Info Br (Code 335)
- 1 Prelim Des (Code 420)
- 1 Lab Mgt (Code 320)
- 3 Hull Des (Code 440)

1 CHBUWEPS
(Code RAAD-222)
Attn: Mr. D. Michel

2 CHONR
- 1 Flu Dyn Br (Code 438)

1 CDR, USNOL, White Oak, Md

1 CDR, USNOTS, China Lake

2 CDR, USNOTS, Pasadena Annex (Code P-508)

1 CDR, ARESDEVCOM
Attn: Mech Br, AF Office of Sci Res

1 CDR, W-PADEVDIV, Aircraft Lab
Attn: Mr. W. Mykytow, Dyn Br

10 CDR, ASTIA

1 CHAFSWP

1 SNAME, N.Y.

1 NRC, Canada

1 NRC, Washington

1 ADMIN, U.S. Maritime Adm
Attn: Mr. R.P. Godwin, Acting CHF, Off of Res & Dev

2 DIR, Natl BuStand
- 1 Dr. G.B. Schubauer, CHF, Flu Mech Sec
- 1 Dr. J.M. Frankland, Consultant

2 DIR, Langley Res Ctr, NASA, Hydr Div
- 1 Mr. I.E. Garrick
- 1 Mr. D.J. Marten

3 DIR, DL, SIT, Hoboken
- 1 Mr. C.J. Henry
- 1 Mr. S. Tsakonas

2 DIR, ORL Penn State
- 1 Dr. M. Sevik

3 DIR, Dept of Mech Sci, SW Res Inst San Antonio
- 1 Dr. H.N. Abramson
- 1 Mr. G. Ransleben

2 DIR, Iowa Inst of Hydrau Res, State Univ of Iowa
- 1 Prof. L. Landweber

3 DIR, St Anthony Falls Hydrau Lab, Univ of Minn, Minneapolis
- 1 Prof. B. Silberman
- 1 Mr. J.N. Wetzel

1 DIR, Appl Phys Lab, Johns Hopkins Univ Silver Spring

1 Elec Boat Div, Genl Dyn Corp, Groton
Attn: Mr. Robert McCandliss

2 Stanford Univ, Dept of Math, Stanford
- 1 Dr. B. Perry
- 1 Dr. E.Y. Hsu

Copies

1 Univ of Calif, Dept of Engin, Inst of Engin Res, Berkeley, Attn: Dr. J.V. Wehausen

3 Calif Inst of Tech, Pasadena
- 1 Dr. M.S. Plesset
- 1 Dr. T.Y. Wu
- 1 Dr. A.J. Acosta

3 Mass Inst of Tech, Flu Dyn Res Lab, Cambridge
- 1 Prof. H. Ashley
- 1 Prof. M. Landahl
- 1 Prof. J. Dugundji

1 Midwest Res Inst, Kansas City
Attn: Mr. Zeydel

4 Univ of Mich, Ann Arbor, Dept of Engin Mech
- 1 Prof. Jesse Ormondroyd
- 1 Prof. C.S. Yih

Dept of NAME
- 1 Prof. R.B. Couch, Dir Exp Nav Tank
- 1 Prof. F. Michaelson

1 Prof. H.A. Schade, Hd, Dept of Nav Arch Univ of Calif, Berkeley

1 Prof. A.G. Strandhagen, Dept of Engin Mech Univ of Notre Dame

1 Prof. W.R. Sears, Grad School of Aero Engin, Cornell Univ, Ithaca

1 Prof. J.S. McNown, Dean of Engin, Univ of Kansas, Lawrence

1 Prof. F.A. Biberstein, Hd, Dept of Civil Engin Catholic Univ, Washington

1 Prof. B. Morrill, Chairman, Mech Engin Dept Swarthmore College, Swarthmore

1 Boeing Airplane Co, Seattle
Attn: Mr. M.J. Turner

2 Convair, San Diego
- 1 Mr. A.D. MacLellan, Sys Dyn Gp
- 1 Mr. H.T. Brooke, Hydro Gp

2 Tech Res Gp, Inc, Syosset, Long Island
- 1 Dr. J. Kotik
- 1 Prof. S. Karp

1 The Rand Corp, Santa Monica
Attn: Dr. B. Parkin

2 Cornell Aero Lab, Buffalo
- 1 Dr. Statler
- 1 Mr. R. White

1 Genl Appl Sci Lab, Inc, Westbury, Long Island
Attn: Dr. F. Lane

1 Gibbs and Cox, Inc, N.Y.

2 Grumman Aircraft Engin Corp, Bethpage, Long Island
- 1 Mr. E. Baird
- 1 Mr. C. Squires

1 Grumman Aircraft Engin Corp, Dyn Dev Div Babylon

2 Pres, Hydronautics, Inc, Rockville

1 Lockheed Aircraft Corp, Missiles & Space Div, Palo Alto
Attn: Mr. R.W. Kermeen

Copies

1 Dr. P. Kaplan, Pres, Oceanics, Inc. New York

4 Natl Phys Lab, Feltham, Middlesex, England
- 1 Dir, Ship Div
- 1 Hd, Aerodyn Div
- 1 Mr. A. Silverleaf
- 1 Mr. D.V. Hilborne

2 DIR, Royal Aircraft Estab Farnborough, Hants, England
Attn: Mr. M.O.W. Wolfe

1 Dr. R. Timman, Natl Luchtvoortlaboratorium Slaterwag 145, Amsterdam, The Netherlands

David Taylor Model Basin. Report 1442.
HYDROELASTIC INSTABILITY OF A CONTROL SURFACE, by D.A. Jewell and Michael E. McCormick. Dec 1961. v, 63p. illus., graphs, refs. UNCLASSIFIED

Initial evidence of flutter of a fully submerged hydrofoil of small aspect ratio under controlled experimental conditions is presented. The influence of several primary parameters on flutter was investigated. Theodorsen's two-dimensional, unsteady flutter theory yielded flutter speed predictions in good agreement with experimental data. Based on the findings, some conditions under which flutter of displacement or hydrofoil craft could be anticipated are discussed.

1. Control surfaces--Flutter-Mathematical analysis
2. Control surfaces--Flutter-Test methods
3. Ship hulls--Vibration--Sources

I. Jewell, D.A.
II. McCormick, Michael E.
III. S-F013 02 01

David Taylor Model Basin. Report 1442.
HYDROELASTIC INSTABILITY OF A CONTROL SURFACE, by D.A. Jewell and Michael E. McCormick. Dec 1961. v, 63p. illus., graphs, refs. UNCLASSIFIED

Initial evidence of flutter of a fully submerged hydrofoil of small aspect ratio under controlled experimental conditions is presented. The influence of several primary parameters on flutter was investigated. Theodorsen's two-dimensional, unsteady flutter theory yielded flutter speed predictions in good agreement with experimental data. Based on the findings, some conditions under which flutter of displacement or hydrofoil craft could be anticipated are discussed.

1. Control surfaces--Flutter-Mathematical analysis
2. Control surfaces--Flutter-Test methods
3. Ship hulls--Vibration--Sources

I. Jewell, D.A.
II. McCormick, Michael E.
III. S-F013 02 01

David Taylor Model Basin. Report 1442.
HYDROELASTIC INSTABILITY OF A CONTROL SURFACE, by D.A. Jewell and Michael E. McCormick. Dec 1961. v, 63p. illus., graphs, refs. UNCLASSIFIED

Initial evidence of flutter of a fully submerged hydrofoil of small aspect ratio under controlled experimental conditions is presented. The influence of several primary parameters on flutter was investigated. Theodorsen's two-dimensional, unsteady flutter theory yielded flutter speed predictions in good agreement with experimental data. Based on the findings, some conditions under which flutter of displacement or hydrofoil craft could be anticipated are discussed.

1. Control surfaces--Flutter-Mathematical analysis
2. Control surfaces--Flutter-Test methods
3. Ship hulls--Vibration--Sources

I. Jewell, D.A.
II. McCormick, Michael E.
III. S-F013 02 01

David Taylor Model Basin. Report 1442.
HYDROELASTIC INSTABILITY OF A CONTROL SURFACE, by D.A. Jewell and Michael E. McCormick. Dec 1961. v, 63p. illus., graphs, refs. UNCLASSIFIED

Initial evidence of flutter of a fully submerged hydrofoil of small aspect ratio under controlled experimental conditions is presented. The influence of several primary parameters on flutter was investigated. Theodorsen's two-dimensional, unsteady flutter theory yielded flutter speed predictions in good agreement with experimental data. Based on the findings, some conditions under which flutter of displacement or hydrofoil craft could be anticipated are discussed.

1. Control surfaces--Flutter-Mathematical analysis
2. Control surfaces--Flutter-Test methods
3. Ship hulls--Vibration--Sources

I. Jewell, D.A.
II. McCormick, Michael E.
III. S-F013 02 01

David Taylor Model Basin. Report 1442.
HYDROELASTIC INSTABILITY OF A CONTROL SURFACE, by D.A. Jewell and Michael E. McCormick. Dec 1961. v, 63p. illus., graphs, refs. UNCLASSIFIED

Initial evidence of flutter of a fully submerged hydrofoil of small aspect ratio under controlled experimental conditions is presented. The influence of several primary parameters on flutter was investigated. Theodorsen's two-dimensional, unsteady flutter theory yielded flutter speed predictions in good agreement with experimental data. Based on the findings, some conditions under which flutter of displacement or hydrofoil craft could be anticipated are discussed.

1. Control surfaces--Flutter-Mathematical analysis
2. Control surfaces--Flutter-Test methods
3. Ship hulls--Vibration--Sources
I. Jewell, D.A.
II. McCormick, Michael E.
III. S-F013 02 01

David Taylor Model Basin. Report 1442.
HYDROELASTIC INSTABILITY OF A CONTROL SURFACE, by D.A. Jewell and Michael E. McCormick. Dec 1961. v, 63p. illus., graphs, refs. UNCLASSIFIED

Initial evidence of flutter of a fully submerged hydrofoil of small aspect ratio under controlled experimental conditions is presented. The influence of several primary parameters on flutter was investigated. Theodorsen's two-dimensional, unsteady flutter theory yielded flutter speed predictions in good agreement with experimental data. Based on the findings, some conditions under which flutter of displacement or hydrofoil craft could be anticipated are discussed.

1. Control surfaces--Flutter-Mathematical analysis
2. Control surfaces--Flutter-Test methods
3. Ship hulls--Vibration--Sources
I. Jewell, D.A.
II. McCormick, Michael E.
III. S-F013 02 01

David Taylor Model Basin. Report 1442.
HYDROELASTIC INSTABILITY OF A CONTROL SURFACE, by D.A. Jewell and Michael E. McCormick. Dec 1961. v, 63p. illus., graphs, refs. UNCLASSIFIED

Initial evidence of flutter of a fully submerged hydrofoil of small aspect ratio under controlled experimental conditions is presented. The influence of several primary parameters on flutter was investigated. Theodorsen's two-dimensional, unsteady flutter theory yielded flutter speed predictions in good agreement with experimental data. Based on the findings, some conditions under which flutter of displacement or hydrofoil craft could be anticipated are discussed.

1. Control surfaces--Flutter-Mathematical analysis
2. Control surfaces--Flutter-Test methods
3. Ship hulls--Vibration--Sources
I. Jewell, D.A.
II. McCormick, Michael E.
III. S-F013 02 01

David Taylor Model Basin. Report 1442.
HYDROELASTIC INSTABILITY OF A CONTROL SURFACE, by D.A. Jewell and Michael E. McCormick. Dec 1961. v, 63p. illus., graphs, refs. UNCLASSIFIED

Initial evidence of flutter of a fully submerged hydrofoil of small aspect ratio under controlled experimental conditions is presented. The influence of several primary parameters on flutter was investigated. Theodorsen's two-dimensional, unsteady flutter theory yielded flutter speed predictions in good agreement with experimental data. Based on the findings, some conditions under which flutter of displacement or hydrofoil craft could be anticipated are discussed.

1. Control surfaces--Flutter-Mathematical analysis
2. Control surfaces--Flutter-Test methods
3. Ship hulls--Vibration--Sources
I. Jewell, D.A.
II. McCormick, Michael E.
III. S-F013 02 01